JOC The Journal of Organic Chemistry

pubs.acs.org/joc Article

# Synthesis of Chrysoporphyrins and a Related Benzopyrene-Fused System

Timothy D. Lash,* Melissa A. Mathius, and Deyaa I. AbuSalim

Cite This: J. Org. Chem. 2022, 87, 16276−16296 Read Online

ACCESS | Metrics & More | Article Recommendations | Supporting Information

**ABSTRACT:** Reaction of 6-nitrochrysene with ethyl isocyanoacetate in the presence of a non-nucleophilic base gave a *c*-annulated pyrrole ethyl ester that was used to prepare chrysene-fused tripyrranes and a chrysopyrrole dialdehyde. Chrysene-fused tripyrranes were reacted with a pyrrole dialdehyde, but poor yields of chrysoporphyrins were obtained. However, condensation of the chrysopyrrole dialdehyde with a series of tripyrranes afforded excellent yields of chrysoporphyrins and an acenaphtho-chrysoporphyrin. Iron(III) chloride mediated oxidative cyclization of a dihexylchrysoporphyrin afforded a benzopyrene-fused porphyrin that exhibited a strongly red-shifted electronic absorption spectrum. DFT calculations show that both chrysoporphyrins and the benzopyrene-fused porphyrin have tautomers that possess 34$\pi$ electron delocalization pathways that pass through the porphyrin nucleus and the fused polycyclic aromatic hydrocarbon (PAH) units. Protonation gave dications that favor 36-atom 34$\pi$ electron circuits. *c*-Annulated pyrrole dialdehydes were also condensed with a carbatripyrrin to generate PAH-fused carbaporphyrins that retained fully aromatic properties.

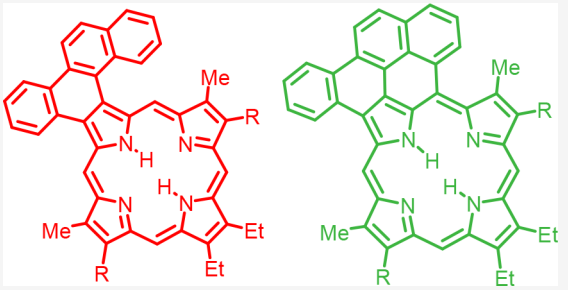




## INTRODUCTION

Polycyclic benzenoid aromatic structures (nanographenes) have received considerable attention[1] due to potential applications in molecular electronics, optoelectronics, photovoltaics, sensing, bioimaging, and therapeutics.[2−4] Furthermore, nanographenes with embedded heterocyclic units are also being investigated for similar applications,[5] including porphyrinoid systems with polycyclic aromatic hydrocarbon (PAH) units[6] such as tetranaphthoporphyrins **1**,[7] tetraphenanthroporphyrins **2**,[8] tetraanthroporphyrins **3**,[9] and tetraacenaphthoporphyrins **4**[10] (Figure 1). Although the parent structures are highly insoluble, the introduction of *meso*-aryl substituents greatly improves their solubility. The discovery that some nitroaromatic compounds, such as 9-nitrophenanthrene, undergo Barton−Zard-type condensations[11−13] with isocyanoacetate esters in the presence of non-nucleophilic bases to afford pyrrole esters with fused aromatic rings (Scheme 1) has provided access to intermediates that can generate numerous classes of annulated porphyrinoids.[14] Porphyrins with fused aromatic moieties include benzoporphyrins **5**,[6] naphtho[1,2-*b*]porphyrins **6**,[7] naphtho[2,3-*b*]porphyrins,[15,16] phenanthroporphyrins **7**,[17] acenaphthoporphyrins **8**,[18] fluoranthoporphyrins **9**, and corannulenoporphyrins **10** (Figure 2),[14,19] and numerous examples of porphyrins with two or more fused rings have also been described.[19] This strategy has also been applied to the preparation of PAH-fused carbaporphyrins, oxypyriporphyrins, oxybenziporphyrins, and heteroporphyrins.[6a,17b] In the present study, the synthesis of porphyrins **7** with fused chrysene units has been investigated. Chrysoporphyrins differ from previously described PAH-fused porphyrinoids because the benzenoid unit is placed in a sterically crowded position that will force the structure to take on a helical orientation. PAH-fused porphyrinoids generally exhibit poor solubility because the planar aromatic structure facilitates strong $\pi$-stacking interactions and the introduction of nonplanar fused chrysene units in **11** could improve the solubility characteristics of this system. In addition, the geometry of **11** is conducive to oxidative cyclization to produce benzopyrene-fused porphyrins **12**. The synthesis, metalation, aromatic characteristics, and oxidative cyclization of chrysoporphyrins are reported below.

## RESULTS AND DISCUSSION

Chrysene-fused pyrrole ester **13** was prepared in 47% yield by reacting 6-nitrochrysene with ethyl isocyanoacetate and 1,8-diazabicyclo[5.4.0]undec-7-ene (DBU) in refluxing THF (Scheme 2).[20] Treatment of **13** with potassium hydroxide in ethylene glycol at 200 °C resulted in saponification and decarboxylation of the ethyl ester to generate unsubstituted chrysopyrrole **14**. Reaction of **14** with 2 equiv of

Received: August 4, 2022
Published: December 2, 2022




https://doi.org/10.1021/acs.joc.2c01859
J. Org. Chem. 2022, 87, 16276−16296

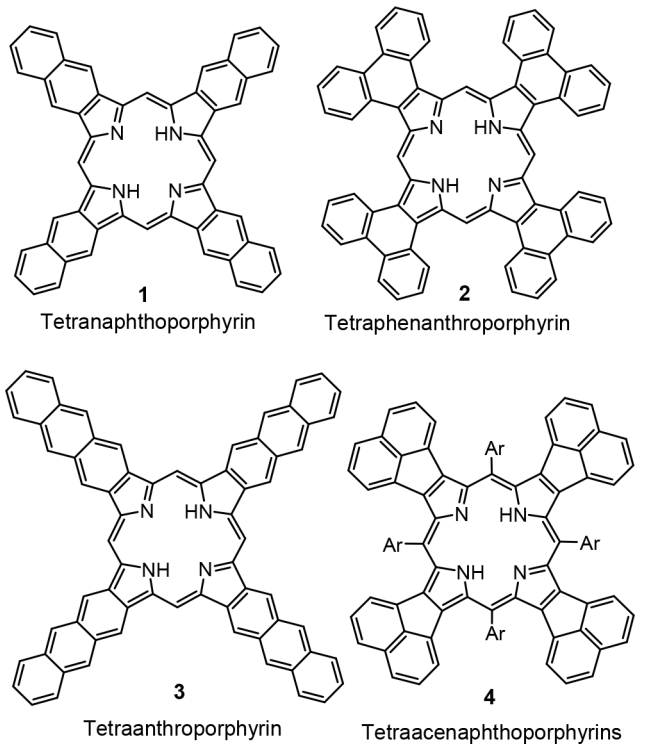


**Figure 1.** Selected examples of porphyrins with four polycyclic aromatic hydrocarbon units.

**Scheme 1. Barton−Zard Synthesis of Phenanthropyrrole Esters**

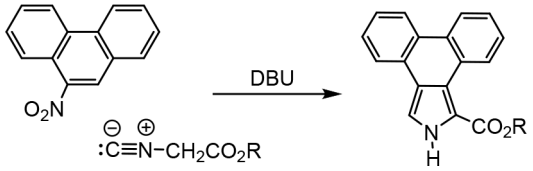


acetoxymethylpyrroles **15** in refluxing ethanol containing acetic acid gave chrysotripyrranes **16**, and these tripyrrolic compounds were investigated as potential precursors to chrysoporphyrins **17** (Scheme 3). Although this strategy has been successfully applied to the synthesis of many PAH-fused porphyrins,[14] including **7**−**10**, mediocre results were obtained using chrysotripyrranes **16**. Tripyrranes **16** were initially treated with trifluoroacetic acid (TFA) for 5 min and, following dilution with dichloromethane, dialdehyde **18** was added. Following oxidation with 2,3-dichloro-5,6-dicyanobenzoquinone (DDQ), poor yields of chrysoporphyrins **17** (<10%) were obtained. In addition, the samples were contaminated with minor impurities even after purification by column chromatography and recrystallization. It was speculated that the chrysene-unit inhibited the required conformation needed for macrocycle formation and the poor results necessitated the development of an alternative route to this system. In our initial '3 + 1' syntheses, the chrysene unit was introduced as a component of the tripyrrane intermediate. In the alternative route, which also uses a '3 + 1' strategy, the PAH unit was incorporated using chrysopyrrole dialdehyde **19** (Scheme 4).

Pyrrole monoaldehydes are easily synthesized using the Vilsmeier−Haack reaction ($POCl_3$-DMF) but it is not possible to prepare pyrrole dialdehydes by this approach. This problem

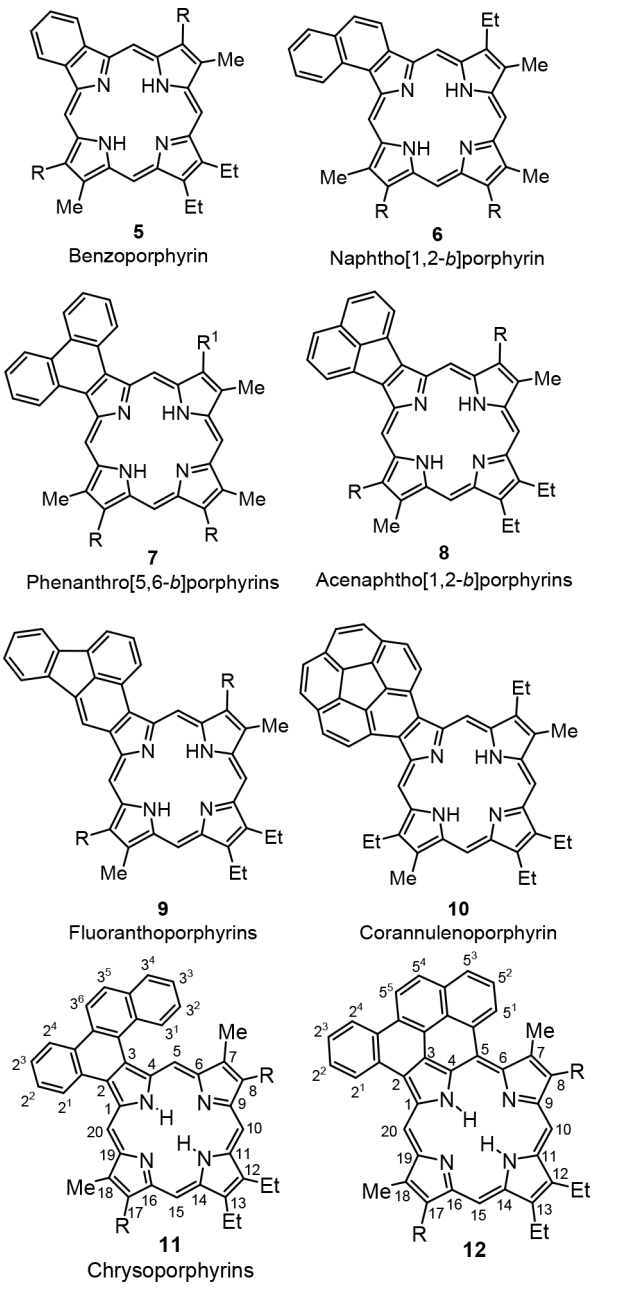


**Figure 2.** Porphyrins with fused aromatic rings.

results from the initially introduced electron-withdrawing aldehyde moiety deactivating the pyrrole nucleus toward electrophilic substitution. However, protection of the aldehyde unit, followed by formylation and deprotection, can allow pyrrole dialdehydes to be accessed.[18] Reaction of chrysopyrrole **14** with $POCl_3$ and DMF, followed by hydrolysis with aqueous sodium hydroxide, gave a mixture of two monoaldehydes, **20a** and **20b**, in a ratio of approximately 3:1. This material could be taken on to the required pyrrole dialdehyde, although the resulting product was impure. 3,4-Dialkylpyrroles have been shown to react with triethyl orthoformate in TFA to directly afford pyrrole dialdehydes,[21] and **14** was reacted under these conditions in an attempt to synthesize **19**. Although the anticipated result was not obtained, this reaction gave an excellent yield of monaldehyde **20a** and only trace amounts of isomer **20b** could be identified. Knoevenagel condensation of **20a** with ethyl cyanoacetate and piperidine[22] in refluxing


https://doi.org/10.1021/acs.joc.2c01859
J. Org. Chem. 2022, 87, 16276−16296

**Scheme 2. Synthesis of Chrysopyrroles**

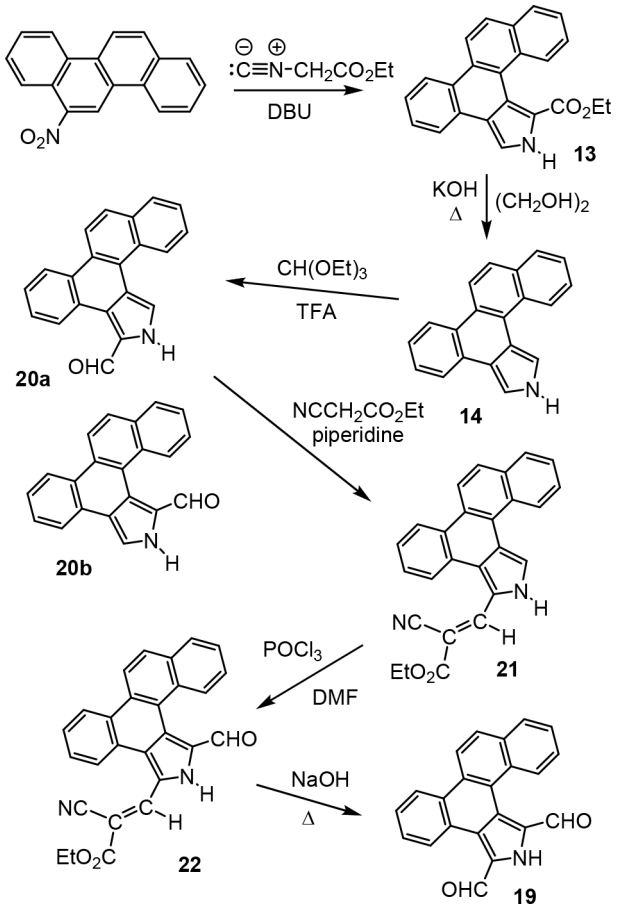


**Scheme 3. Synthesis of Chrysoporphyrins from Chrysotripyrranes**

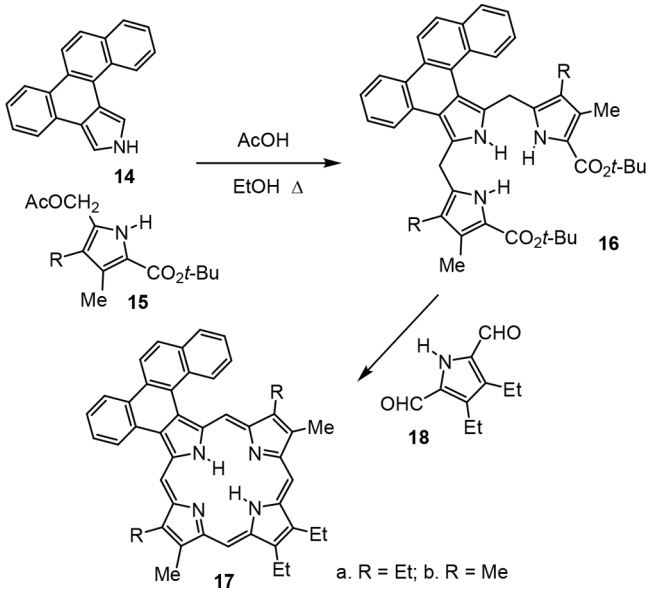


ethanol gave cyanovinyl derivative **21**. Vilsmeier−Haack formylation afforded aldehyde **22**, and subsequent cleavage of the protective group with refluxing aqueous sodium hydroxide solution afforded pure dialdehyde **19**. Although several steps were required to convert **14** into **19**, an overall yield of 78% was obtained.

**Scheme 4. Synthesis of Chrysoporphyrins from a Chrysopyrrole Dialdehyde**

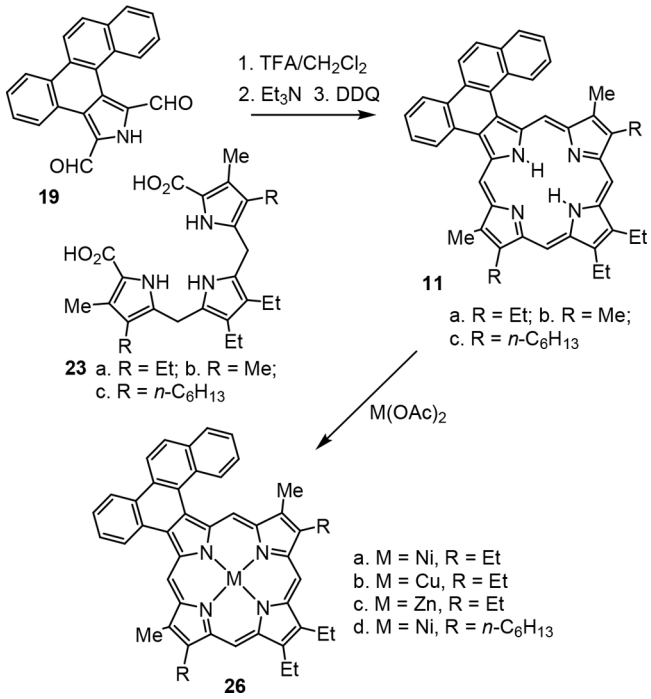


Dialdehyde **19** was condensed with tripyrrane **23a**[23,24] in the presence of TFA and oxidized with DDQ to give pure chrysoporphyrin **11a** in 45% yield (Scheme 4). Unlike porphyrins **7**−**10**, chrysoporphyrin **11a** was sufficiently soluble to obtain proton and carbon-13 NMR spectra. The presence of long-chain alkyl substituents can be used to improve solubility, but this type of substitution was not required in this case. In order to further assess the solubility of chrysoporphyrins, two of the ethyl substituents were replaced by methyl groups. 3,4-Diethylpyrrole was reacted with acetoxymethylpyrrole **24b** and acetic acid in refluxing ethanol to give tripyrrane dibenzyl ester **25b** (Scheme 5), and subsequent cleavage of the protective

**Scheme 5. Synthesis of Tripyrranes**

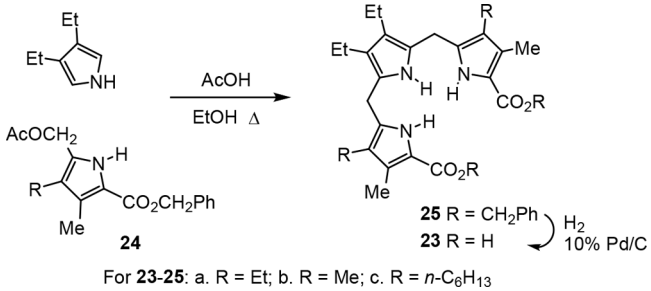


groups with hydrogen over 10% Pd/C afforded the corresponding dicarboxylic acid **23b**. Condensation of **23b** with dialdehyde **19** afforded tetramethylchrysoporphyrin **11b**. Although this porphyrin was less soluble than **11a**, it was still sufficiently soluble to allow a proton NMR spectrum of the free base to be obtained in $CDCl_3$.

The proton NMR spectra for chrysoporphyrins **11** demonstrate that the macrocycles retain fully aromatic characteristics. The proton NMR spectrum of **11a** showed the four strongly deshielded *meso*-proton resonances at 11.27,


https://doi.org/10.1021/acs.joc.2c01859
J. Org. Chem. 2022, 87, 16276−16296

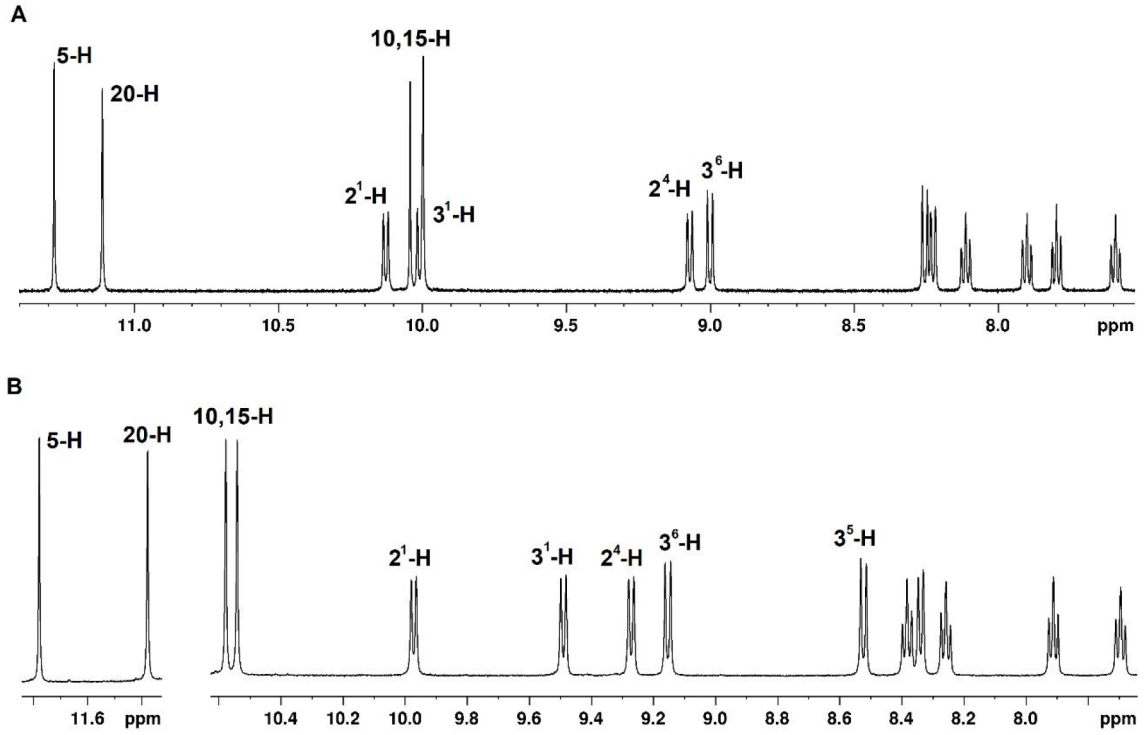


**Figure 3.** Proton NMR spectra of chrysoporphyrin **11a** in $CDCl_3$ (A) and TFA-$CDCl_3$ (dication **11a**$H_2^{2+}$, B).

11.11, 10.04, and 10.00 ppm (Figure 3A), while the chrysene unit gave rise to a series of peaks between 7.5 and 10.2 ppm. Addition of TFA resulted in the formation of the related dication **11a**$H_2^{2+}$, and this species produced further downfield shifts to the *meso*-protons and some significant, mostly smaller, shifts to the chrysene protons (Figure 3B). Porphyrins often exhibit stronger ring current effects for the dications, although the presence of two positive charges also results in deshielding. The presence of a macrocyclic ring current is evident in these spectra, but it was not clear whether the aromatic conjugation pathways extended through the fused benzenoid ring system. An added complication is that the N−H protons within the porphyrin cavity can be placed in 6 different positions so that 6 different tautomers might be present in solution. In order to assess the relative stability and $\pi$-delocalization pathways in these tautomers, density functional theory (DFT) calculations were carried out (Table 1). The pyrrole rings have been assigned as rings *a*, *b*, *c*, and *d*, and these labels are used to designate the positions of the internal protons (e.g., the chrysoporphyrin with internal hydrogens connected to rings *b* and *d* is referred to as **CP**$_{bd}$). Two of the tautomers, **CP**$_{bd}$ and **CP**$_{ac}$, have NHs at opposite positions, and these *trans*-tautomers are significantly more stable than the four *cis*-forms. Tautomer **CP**$_{ac}$ was calculated to be approximately 1.4 kcal/mol less stable than **CP**$_{bd}$. As predicted, the chrysene unit is twisted away from the porphyrin nucleus with dihedral angles of up to 40° (Table 2), although the macrocycle is relatively planar.

The aromatic characteristics of the individual tautomers were assessed using nucleus independent chemical shift calculations (NICS) and related NICS(1)$_{zz}$ calculations.[25] The latter primarily measures the contribution due to the $\pi$-electrons and is considered to be more reliable. In both cases, strongly negative values are consistent with shielding due to an aromatic ring current. Positive values may result from antiaromatic (paratropic) systems or from sites lying external to the aromatic delocalization pathway. All six chrysoporphyrin tautomers exhibit strongly aromatic properties. Focusing on the two most stable tautomers, the NICS(0) values are similar but the conjugation pathways are strikingly different. In **CP**$_{bd}$, ring *a* gives weakly positive results, but in **CP**$_{ac}$ ring *a* has strongly negative NICS and NICS$_{zz}$ values. In addition, in **CP**$_{bd}$ rings *b* and *d* produce larger negative values than ring *c*, but in **CP**$_{ac}$ ring *c* gives a much larger negative value than *b* or *d*. These results strongly imply that the chrysene ring is not involved in the aromatic circuit for **CP**$_{bd}$ but significantly contributes to the aromatic properties for **CP**$_{ac}$. The anisotropy of induced current density (AICD) plots[26] were also used to probe the aromatic properties of the chrysoporphyrin tautomers. As can be seen in Figure 4, tautomer **CP**$_{ac}$ favors the conjugation pathway that involves a circuit that passes through the periphery of the chrysene unit. Calculations were also performed for the related diprotonated chrysoporphyrin dication **CP**$H_2^{2+}$, and the NICS values confirm that the macrocycle is strongly diatropic (Table 1). In this case, rings *a*−*h* all give large negative values, indicating that a [36]-annulene dication pathway is favored for **CP**$H_2^{2+}$ (Figure 5). The 36-atom 34$\pi$-electron circuit is also evident in the AICD plot shown in Figure 4. The chrysene ring is again twisted away from the porphyrin by nearly 40°, but the porphyrin nucleus is also distorted favoring a saddle-shaped conformation due to steric crowding from the presence of four hydrogens within the cavity (Table 2).

The UV−vis spectrum for chrysoporphyrin **9a** gave a Soret band at 425 nm and Q bands at 525, 563, 582, and 638 nm (Figure 6). These values represent only weakly red-shifted absorptions compared to octaalkylporphyrins as has been previously noted for related systems such as phenanthroporphyrins.[19] Spectroscopic titration with TFA led to the formation of a new species, and with 100 equiv of TFA, a


https://doi.org/10.1021/acs.joc.2c01859
J. Org. Chem. 2022, 87, 16276−16296

**Table 1. Calculated Relative Energies and NICS Values for Chrysoporphyrin Tautomers and a Related Dication**

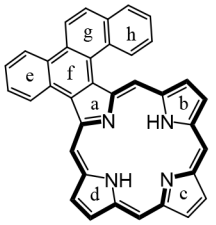


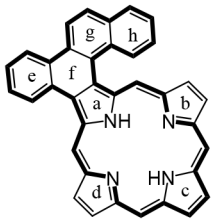


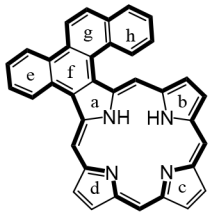


| | $CP_{bd}$ | $CP_{ac}$ | $CP_{ab}$ |
|---|---|---|---|
| $\Delta E$ | 0.00 | 1.43 | 10.05 |
| $\Delta G_{298}$ | 0.00 | 1.42 | 9.97 |
| *NICS(0) \| NICS($1_{zz}$)* | -14.11 \| -36.39 | -13.87 \| -32.78 | -14.08 \| -35.69 |
| *NICS(a) \| NICS($a_{zz}$)* | +2.47 \| +0.70 | -7.05 \| -16.12 | -8.82 \| -24.27 |
| *NICS(b) \| NICS($b_{zz}$)* | -12.21 \| -21.70 | -2.79 \| -6.94 | -12.90 \| -38.74 |
| *NICS(c) \| NICS($c_{zz}$)* | -2.91 \| -14.69 | -12.73 \| -32.37 | -2.13 \| -13.07 |
| *NICS(d) \| NICS($d_{zz}$)* | -12.11 \| -38.23 | -2.63 \| -19.55 | -2.13 \| -12.31 |
| *NICS(e) \| NICS($e_{zz}$)* | -7.05 \| -19.77 | -7.21 \| -20.69 | -7.05 \| -21.46 |
| *NICS(f) \| NICS($f_{zz}$)* | -2.89 \| -10.77 | -2.46 \| -9.60 | -1.84 \| -11.40 |
| *NICS(g) \| NICS($g_{zz}$)* | -4.84 \| -15.67 | -4.98 \| -15.94 | -4.92 \| -17.09 |
| *NICS(h) \| NICS($h_{zz}$)* | -7.44 \| -27.20 | -7.42 \| -27.21 | -7.18 \| -12.01 |

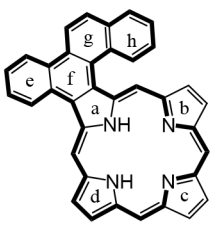


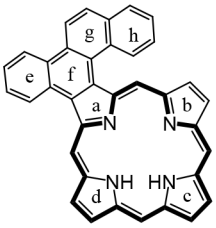


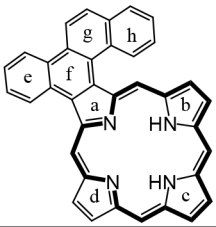


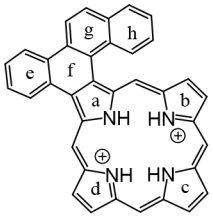


| | $CP_{ad}$ | $CP_{cd}$ | $CP_{bc}$ | $CPH_2^{2+}$ |
|---|---|---|---|---|
| $\Delta E$ | 10.91 | 8.40 | 8.53 | |
| $\Delta G_{298}$ | 10.97 | 8.12 | 8.64 | |
| *NICS(0) \| NICS($1_{zz}$)* | -13.71 \| -32.31 | -14.11 \| -33.34 | -14.08 \| -32.97 | -13.50 \| -33.60 |
| *NICS(a) \| NICS($a_{zz}$)* | -7.55 \| -16.84 | +3.13 \| +2.08 | +3.24 \| +2.57 | -9.93 \| -24.11 |
| *NICS(b) \| NICS($b_{zz}$)* | -2.26 \| -6.13 | -2.28 \| -5.92 | -12.65 \| -22.63 | -13.45 \| -48.20 |
| *NICS(c) \| NICS($c_{zz}$)* | -2.35 \| -13.51 | -12.60 \| -31.79 | -12.75 \| -31.74 | -13.61 \| -22.11 |
| *NICS(d) \| NICS($d_{zz}$)* | -12.69 \| -39.49 | -12.57 \| -37.79 | -2.14 \| -19.47 | -13.01 \| -43.46 |
| *NICS(e) \| NICS($e_{zz}$)* | -7.31 \| -20.35 | -6.96 \| -20.43 | -7.09 \| -19.83 | -8.24 \| -23.54 |
| NICS(f) \| NICS($f_{zz}$) | -2.51 \| -9.29 | -2.87 \| -11.34 | -2.99 \| -10.86 | -4.16 \| -15.86 |
| NICS(g) \| NICS($g_{zz}$) | -4.99 \| -16.16 | -4.78 \| -15.58 | -4.78 \| -15.42 | -4.45 \| -17.46 |
| NICS(h) \| NICS($h_{zz}$) | -7.46 \| -27.28 | -7.39 \| -27.16 | -7.43 \| -27.09 | -7.51 \| -14.43 |

diminished Soret band was observed at 422 nm together with weaker absorptions at 574 and 626 nm. At much higher concentrations of TFA, further spectroscopic changes were observed. Specifically, in 5% TFA the Soret band shifted to 412 nm, although the weaker bands were much less effected. Porphyrins usually directly form diprotonated species, and the results from the titration may indicate the formation of a dication without any significant buildup of a monoprotonated species (based upon the presence of clear isosbestic points). The changes occurring at higher concentrations of TFA are harder to interpret but may be due to hydrogen bonding interactions.

Chrysoporphyrin **11a** was reacted with nickel(II), copper(II), and zinc acetate to give the related metalloporphyrins **26a–c** in 83–96% yield (Scheme 4). Nickel(II) porphyrin **26a** gave a Soret band at 419 nm and weaker absorptions at 540 and 586 nm (Figure 7). The proton NMR spectrum shows that the complex is aromatic, but the *meso*-protons are not as far downfield, ranging from 9.58 to 10.56 ppm, indicating that there is a small reduction in the diamagnetic ring current. Copper(II) complex **26b** similarly gave a Soret band at 419 nm and Q bands at 546 and 593 nm (Figure 7). Unfortunately, copper(II) porphyrins are paramagnetic and it was not possible to obtain useful NMR data for this derivative. Zinc complex **26c** proved to be a highly insoluble green solid, but proton NMR spectra could be obtained in DMSO-$d_6$ or $CDCl_3$ containing pyrrolidine. In DMSO-$d_6$, the *meso*-protons were observed at 11.14, 11.12, 10.04, and 9.99 ppm, indicating that this complex has similar diatropic properties to the parent free base porphyrin **11a**. The UV–vis spectrum of **11a** in 1% pyrrolidine-chloroform gave bathochromically shifted absorptions with a Soret band at 440 nm. These results are consistent with other ring fused metalloporphyrins,[19] and the reduced diatropicity of the nickel complex can be attributed to the macrocycle twisting to coordinate to the relatively small nickel(II) cation.

Given the improved solubility characteristics of chrysoporphyrins, the synthesis of a related chryso-acenaphthoporphyrin **27** was investigated (Scheme 6). Acenaphthoporphyrins **8** exhibit highly modified UV–vis spectra with strongly red-shifted absorptions[18] but often have poor solubility. Acenaphthotripyrrane **28** was treated with TFA and condensed with chrysopyrrole dialdehyde **19** to give, following oxidation with DDQ, the *opp*-chryso-acenaphthoporphyrin **27**. Although this


https://doi.org/10.1021/acs.joc.2c01859
J. Org. Chem. 2022, 87, 16276–16296

**Table 2. Calculated Dihedral Angles for Chrysoporphyrin and Benzopyrenoporphyrin Tautomers, and Related Dications**

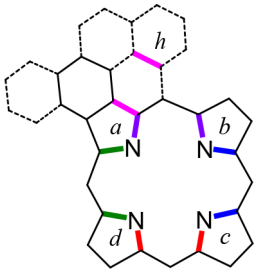


| | ab | bc | cd | da | ah | average dihedral |
|---|---|---|---|---|---|---|
| $CP_{ac}$ | -6.30 | 1.86 | 0.70 | -6.31 | -36.08 | 10.25 |
| $CP_{bd}$ | -6.38 | 1.37 | 1.04 | -6.89 | -34.64 | 10.06 |
| $CP_{ab}$ | -6.63 | 2.44 | 2.92 | 1.85 | -40.63 | 10.89 |
| $CP_{ad}$ | -5.03 | 2.00 | 1.32 | -8.85 | -34.80 | 10.40 |
| $CP_{cd}$ | -8.42 | 1.47 | 0.19 | -4.07 | -35.01 | 9.83 |
| $CP_{bc}$ | -4.36 | 1.46 | 1.06 | -9.54 | -34.29 | 10.14 |
| $CPH_2^{2+}$ | -21.27 | 18.92 | -19.22 | 19.94 | -39.35 | 23.74 |
| $BPP_{ac}$ | -9.52 | 7.97 | 1.02 | -2.74 | -1.40 | 4.53 |
| $BPP_{bd}$ | 5.14 | -6.33 | -1.65 | 5.54 | 1.32 | 4.00 |
| $BPP_{ab}$ | 11.31 | -7.27 | -2.82 | 2.00 | 1.46 | 4.97 |
| $BPP_{ad}$ | -7.11 | 8.11 | 1.07 | -5.29 | -1.17 | 4.55 |
| $BPP_{cd}$ | -10.85 | 7.53 | 2.03 | -2.29 | -0.94 | 4.73 |
| BPPbc | 3.04 | -6.10 | -0.76 | 7.01 | 1.46 | 3.67 |
| $BPPH_2^{2+}$ | -26.73 | -24.96 | -16.36 | 18.85 | -1.59 | 17.70 |

represents a new $\pi$-extended porphyrin, the solubility characteristics were disappointing. The NMR spectra could only be obtained in TFA-$CDCl_3$ for the protonated species, but these results did show that the porphyrin dication was fully aromatic and the *meso*-protons were observed downfield at 11.74, 11.33, 10.99, and 10.95 ppm. The UV−vis spectrum for **27** gave a Soret band at 440 nm and Q bands at 591, 621, 657, and 684 nm (Figure 8). However, the longer wavelength absorptions were relatively weak. Titration with TFA resulted in the formation of a new species with a Soret band at 464 nm that was attributed to the formation of a dicationic species (Figure 8). No significant changes were observed at higher concentrations of TFA.

The orientation of the chrysene ring in chrysoporphyrins **11** suggested that it might be possible to oxidatively ring close the structure (Scholl reaction) to give benzopyrene-fused porphyrins **12** (Scheme 7). However, this would also result in the formation of a comparatively planar porphyrin structure that would most likely be relatively insoluble in organic solvents. In order to address this issue, a tripyrrane **25c** with two hexyl side chains was synthesized. Reaction of 1-iodohexane with 2,4-pentanedione and potassium carbonate in refluxing acetone gave 3-hexyl-2,4-pentanedione (**30**) and this was condensed with diethyl aminomalonate (**31**) in refluxing acetic acid to produce hexyl substituted pyrrole **32** (Scheme 8). Transesterification with sodium benzyloxide in benzyl alcohol afforded the corresponding benzyl ester **33**, and this was reacted with lead tetraacetate to give acetoxymethylpyrrole **24c**. A 2 equiv amount of **24c** reacted with 3,4-diethylpyrrole and acetic acid in refluxing ethanol to give tripyrrane **25c** (Scheme 5). The benzyl ester protective groups were then cleaved with hydrogen over 10% Pd/C to generate the related dicarboxylic acid **23c**. In order to assess the effectiveness of introducing hexyl substituents, a dihexyl

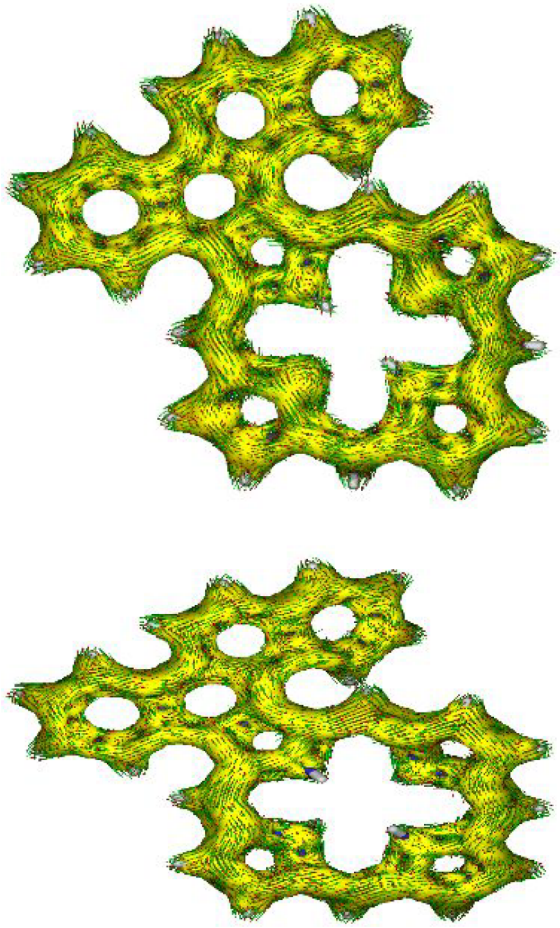

**Figure 4.** AICD plots (isovalues = 0.05) of chrysoporphyrin tautomer $CP_{ac}$ (top) and dication $CPH_2^{2+}$ (bottom).

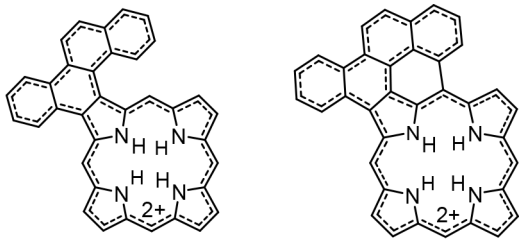


$CPH_2^{2+}$ $BPPH_2^{2+}$

**Figure 5.** 34$\pi$ electron delocalization pathways in chrysoporphyrin and benzopyrenoporphyrin dications.

pyrenoporphyrin **34** was prepared (Scheme 9). In an earlier study, a series of pyrenoporphyrins were synthesized,[27] but these proved to be highly insoluble. Tripyrrane **23c** was condensed with pyrenopyrrole dialdehyde **35** under standard '3 + 1' conditions to give pyrenoporphyrin **34** in 32% yield (Scheme 9). The UV−vis spectrum for **35** (Figure 9) gave a Soret band at 419 nm and Q bands at 519, 558, 579, and 634 nm. Spectroscopic titration with TFA led to the formation of a new species, attributed to the corresponding dication $34H_2^{2+}$, with Soret bands at 421 and 434 nm. The solubility of **34** was considerably improved, and proton and carbon-13 NMR spectra were easily obtained. In the proton NMR spectrum for free base **34**, the *meso*-protons gave rise to two 2H singlets at



https://doi.org/10.1021/acs.joc.2c01859
J. Org. Chem. 2022, 87, 16276−16296

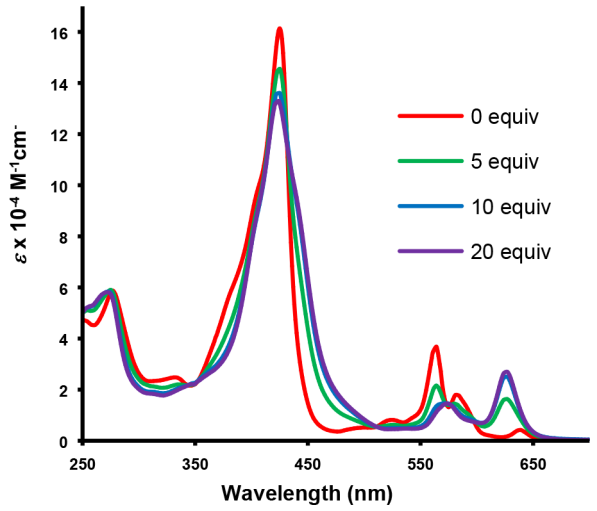


**Figure 6.** UV−vis spectra of chrysoporphyrin **11a** in $CH_2Cl_2$ and with 5, 10, and 20 equiv of TFA showing the formation of a protonated species.

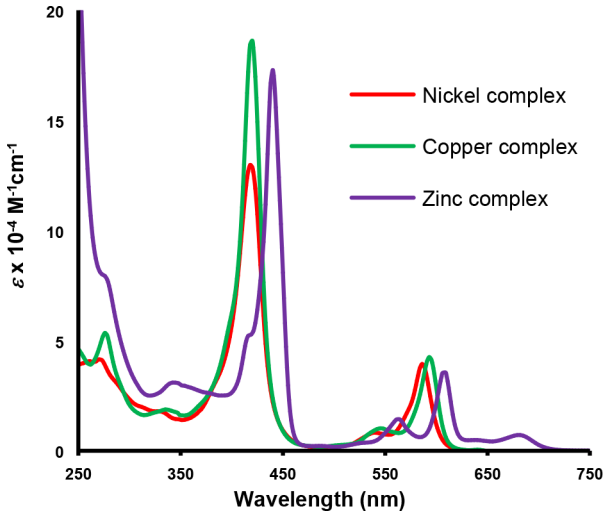


**Figure 7.** UV−vis spectra of nickel(II) and copper(II) chrysoporphyrins **26a** and **26b** in chloroform, and zinc complex **26c** in 1% pyrrolidine-chloroform.

**Scheme 6. Synthesis of an Acenaphtho-Chrysoporphyrin**

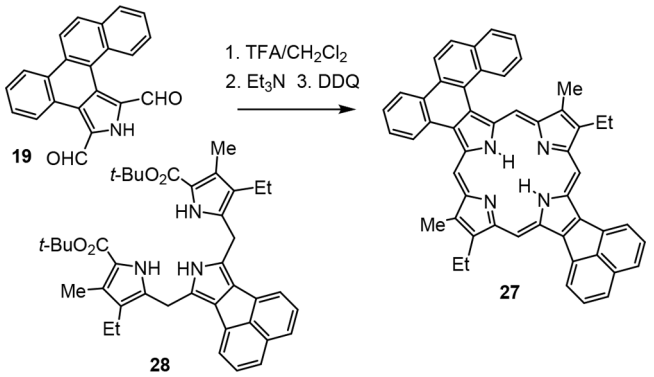


11.59 and 9.86 ppm, confirming the presence of a strong diatropic ring current.

Reaction of tripyrrane **23c** with chrysopyrrole dialdehyde **19** gave dihexyl-chrysoporphyrin **11c** in 45% yield (Scheme 4).

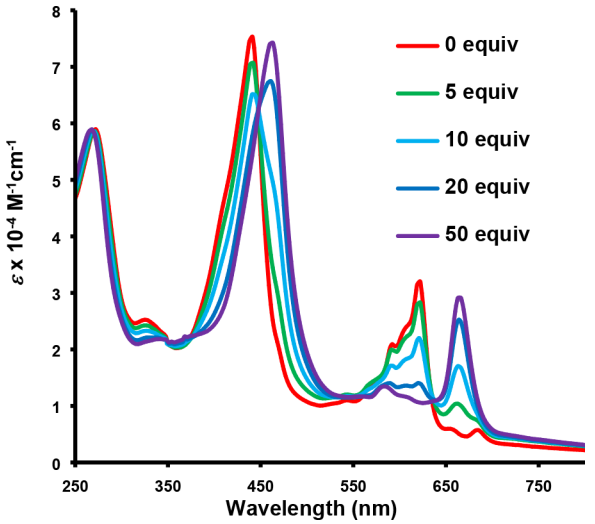


**Figure 8.** UV−vis spectra of acenaphtho-chrysoporphyrin **27** in chloroform, and with 5, 10, 20, and 50 equiv of TFA.

**Scheme 7. Oxidative Ring Closure of Chrysoporphyrins**

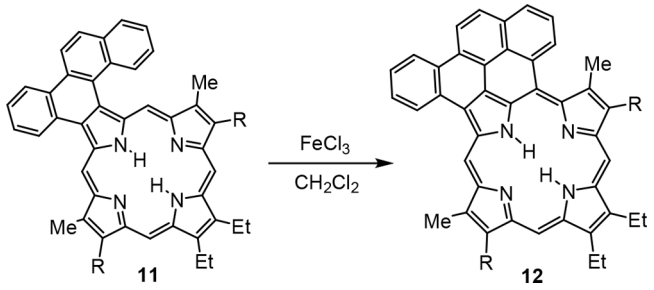


**Scheme 8. Synthesis of Hexyl Substituted Pyrrolic Intermediates**

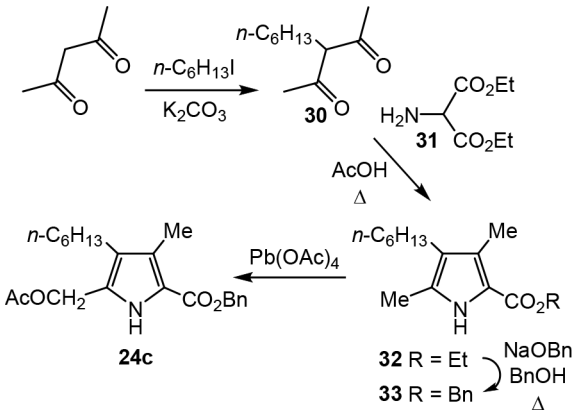


The spectroscopic properties were mostly similar to those obtained for **11a** and **11b**, and the UV−vis spectra for **11c** in $CH_2Cl_2$ or in 5% TFA-$CH_2Cl_2$ were virtually identical to those for **11a**. However, the spectroscopic titration of **11c** revealed significant differences (see Supporting Information). The porphyrin appeared to be less basic, as it required more equivalents of TFA to form the protonated species. In addition, a new peak was observed at 598 nm in spectra run with 100−300 equiv of TFA. The origins of these differences are not clear, but they may result from the long chain hexyl groups interfering with hydrogen bonding interactions to the excess TFA.



https://doi.org/10.1021/acs.joc.2c01859
J. Org. Chem. 2022, 87, 16276−16296

**Scheme 9. Synthesis of a Pyrenoporphyrin**

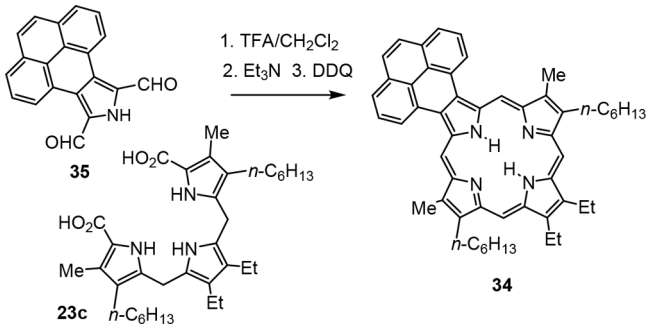


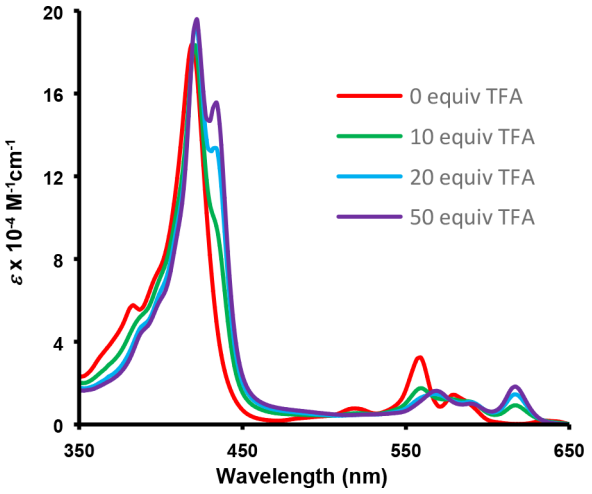


**Figure 9.** UV−vis spectra of pyrenoporphyrin **34** in chloroform, and with 10, 20, and 50 equiv of TFA.

Scholl reactions with porphyrins have been well studied[28] and are often carried out on metalated derivatives. However, in our hands the dihexyl-substituted nickel(II) complex **26d** failed to cyclize with a variety of reagents including ferric chloride, DDQ, $Sc(OTf)_3$-DDQ,[28] and nitrosonium tetrafluoroborate.[29] Similarly, no cyclization was observed for free base porphyrin **11c** under most of these conditions. Fortunately, reaction of **11c** with ferric chloride proved to be the exception. Even so, anhydrous conditions led to a considerable amount of decomposition and good results could only obtained using $FeCl_3 \cdot 6H_2O$ in refluxing dichloromethane. Following purification by column chromatography and recrystallization, **12c** was obtained in 64% yield (Scheme 7). Chrysoporphyrin **11a** also reacted under these conditions, but the product, presumed to be **12a**, was too insoluble to allow spectroscopic characterization. Ferric chloride can act as a Lewis acid catalyst as well as an oxidant. Coordination of $FeCl_3$ to one of the nitrogens would activate the porphyrin system toward nucleophilic attack, and this may initiate intramolecular electrophilic aromatic substitution of the chrysene unit to form the observed six-membered ring (Scheme 10). In conjunction with a second equivalent of $FeCl_3$, a two-electron oxidation step would then take place thereby generating the benzopyrenoporphyrin **12**.

The UV−vis spectrum gave a strongly red-shifted Soret band at 467 nm together with Q bands at 558, 608, and 683 nm (Figure 10). Spectrophotometric titration with TFA led to the formation of a new species that was attributed to dication $\mathbf{12c}H_2^{2+}$. This gave a Soret band at 486 nm and a weaker

**Scheme 10. Proposed Mechanism for the Formation of Benzopyrenoporphyrins**

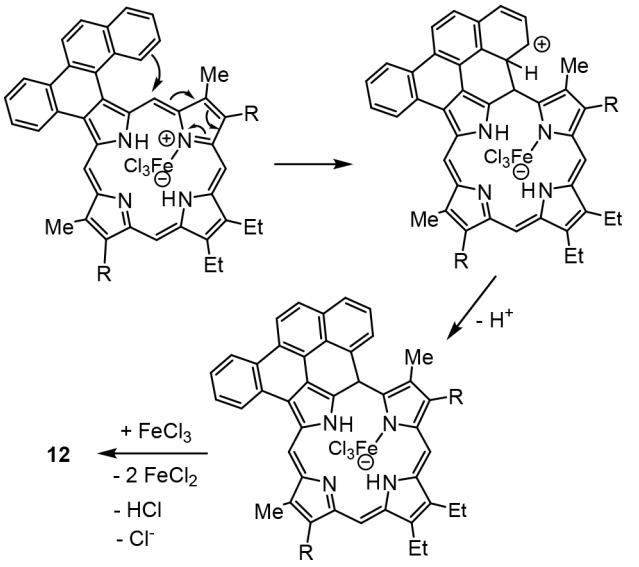


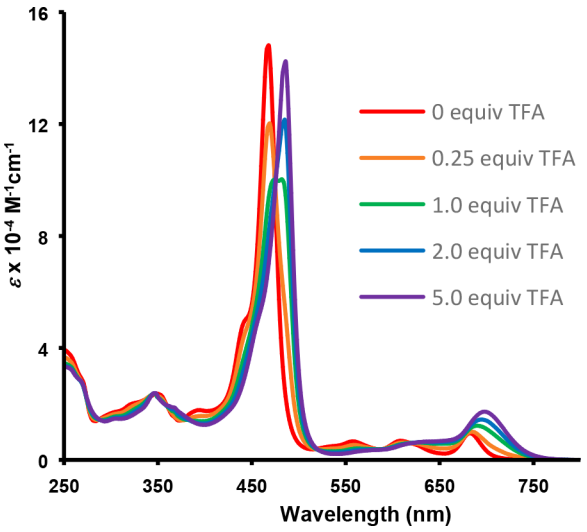


**Figure 10.** UV−vis spectra of benzopyrenoporphyrin **12c** in chloroform, and with 0.25, 1, 2, and 5 equiv of TFA.

absorption at 700 nm. The data indicate that **12c** is significantly more basic than chrysoporphyrins **11**, and this can be attributed to flattening of the macrocycle, as this aids change delocalization in the protonated forms. Further addition of TFA led to minor shifts, but these were not consistent with the formation of further protonated species. Benzopyrenoporphyrin **12c** was sufficiently soluble to obtain a proton NMR spectrum in $CDCl_3$ (Figure 11A). Three 1H singlets were observed for the *meso*-protons at 10.78, 10.08, and 9.81 ppm, again demonstrating that this system has global aromatic properties. In TFA-$CDCl_3$, the *meso*-protons were shifted further downfield giving three 1H singlets at 10.93, 10.33, and 9.88 ppm (Figure 11B). Although the aromatic character of the free base and protonated forms was unambiguously confirmed from these results, it was unclear whether the fused PAH-unit was significantly involved. Analysis of the results was further complicated by the fact that six tautomers of benzopyrenoporphyrin (**BPP**) with two internal NH protons are possible (Table 3). In terms of


https://doi.org/10.1021/acs.joc.2c01859
J. Org. Chem. 2022, 87, 16276−16296

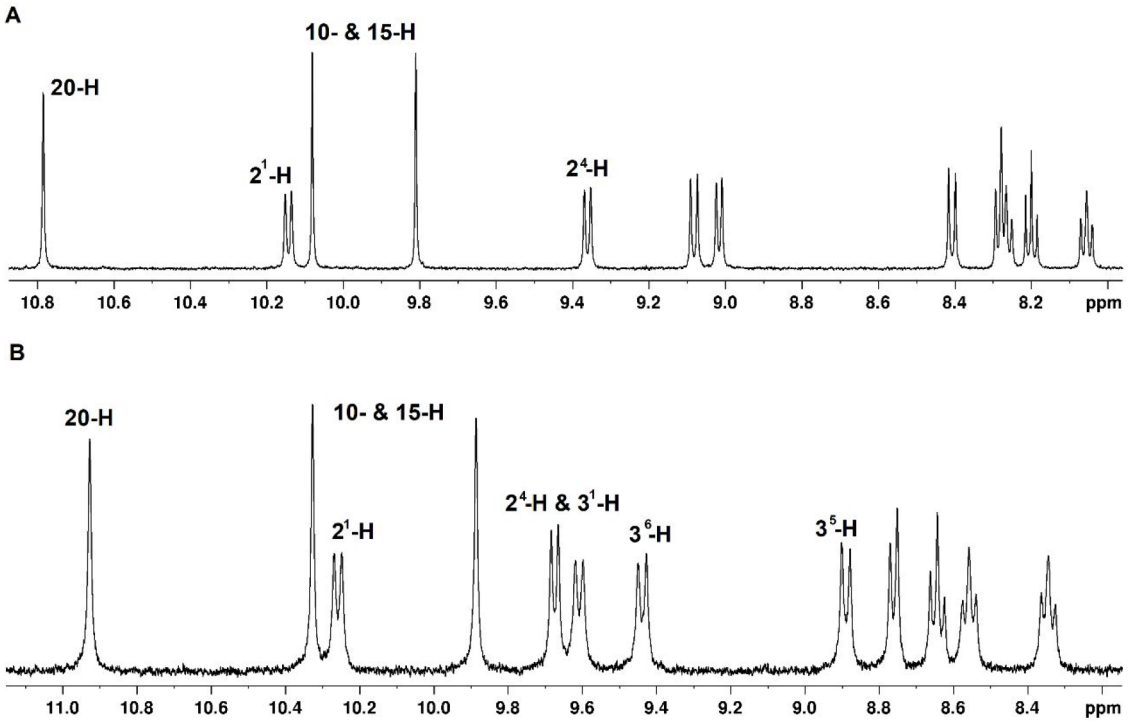


**Figure 11.** Proton NMR spectra of benzopyrene-fused porphyrin **12c** in $CDCl_3$ (A) and TFA-$CDCl_3$ (dication **12c**$H_2^{2+}$; B).

**Table 3. Calculated Relative Energies and NICS Values for Benzopyrenoporphyrin Tautomers and a Related Dication**

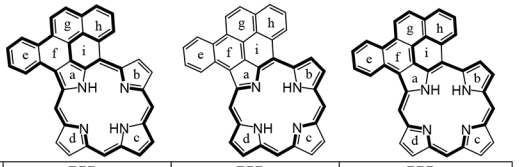

| | **BPP**$_{ac}$ | **BPP**$_{bd}$ | **BPP**$_{ab}$ |
|---|---|---|---|
| $\Delta E$ | 0.82 | 0.00 | 9.98 |
| $\Delta G_{298}$ | 0.60 | 0.00 | 9.86 |
| *NICS(0) \| NICS*($1_{zz}$) | -12.00 \| -30.04 | -13.39 \| -32.99 | -11.61 \| -28.98 |
| *NICS(a) \| NICS*($a_{zz}$) | -6.02 \| -15.81 | +1.83 \| -2.83 | -6.45 \| -16.00 |
| *NICS(b) \| NICS*($b_{zz}$) | -2.39 \| -20.98 | -12.54 \| -41.60 | -13.37 \| -43.45 |
| *NICS(c) \| NICS*($c_{zz}$) | -13.04 \| -34.43 | 2.97 \| -16.20 | -2.54 \| -15.18 |
| *NICS(d) \| NICS*($d_{zz}$) | -2.45 \| -10.39 | -11.05 \| -24.69 | -1.41 \| -7.85 |
| *NICS(e) \| NICS*($e_{zz}$) | -8.41 \| -29.37 | -7.93 \| -28.35 | -8.38 \| -29.51 |
| *NICS(f) \| NICS*($f_{zz}$) | -6.84 \| -21.10 | -6.17 \| -19.59 | -6.83 \| -21.01 |
| *NICS(g) \| NICS*($g_{zz}$) | -4.81 \| -16.05 | -4.70 \| -15.**67** | -4.94 \| -15.82 |
| *NICS(h) \| NICS*($h_{zz}$) | -8.26 \| -20.81 | -7.80 \| -19.41 | -8.32 \| -20.24 |
| *NICS(i) \| NICS*($i_{zz}$) | +4.24 \| +9.54 | +5.26 \| +11.31 | +4.14 \| +10.45 |

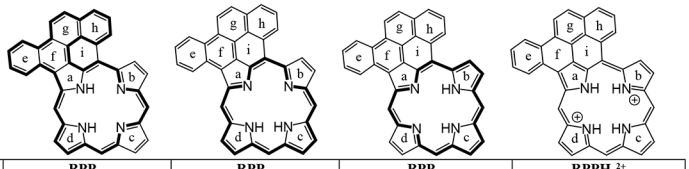

| | **BPP**$_{ad}$ | **BPP**$_{cd}$ | **BPP**$_{bc}$ | **BPPH**$_2^{2+}$ |
|---|---|---|---|---|
| $\Delta E$ | 9.99 | 9.09 | 8.95 | |
| $\Delta G_{298}$ | 9.61 | 8.80 | 8.67 | |
| *NICS(0) \| NICS*($1_{zz}$) | -12.35 \| -31.12 | -12.87 \| -31.22 | -13.61 \| -34.33 | -9.05 \| -20.79 |
| *NICS(a) \| NICS*($a_{zz}$) | -6.90 \| -18.04 | +2.44 \| +0.45 | +2.60 \| -1.52 | -11.25 \| -26.38 |
| *NICS(b) \| NICS*($b_{zz}$) | -1.27 \| -17.62 | -2.53 \| -0.60 | -12.72 \| -40.55 | -13.43 \| -44.14 |
| *NICS(c) \| NICS*($c_{zz}$) | -3.23 \| -15.61 | -13.46 \| -31.97 | -12.37 \| -33.08 | -10.93 \| -18.53 |
| *NICS(d) \| NICS*($d_{zz}$) | -12.44 \| -27.76 | -11.12 \| -32.15 | -1.25 \| -7.87 | -9.42 \| -33.45 |
| *NICS(e) \| NICS*($e_{zz}$) | -8.43 \| -29.66 | -7.88 \| -23.35 | -7.86 \| -28.13 | -8.98 \| -26.99 |
| *NICS(f) \| NICS*($f_{zz}$) | -6.75 \| -21.16 | -6.24 \| -18.56 | -6.08 \| -19.66 | -4.27 \| -13.91 |
| *NICS(g) \| NICS*($g_{zz}$) | -4.56 \| -15.86 | -4.96 \| -19.04 | -4.44 \| -15.61 | -4.29 \| -15.35 |
| *NICS(h) \| NICS*($h_{zz}$) | -8.06 \| -21.42 | -8.08 \| -30.16 | -7.62 \| -19.94 | -7.51 \| -22.04 |
| *NICS(i) \| NICS*($i_{zz}$) | +4.32 \| +9.31 | +4.84 \| +6.12 | +5.45 \| +11.27 | -1.79 \| -5.13 |

relative energies, DFT calculations showed that the *trans*-isomers were more stable than the *cis*-isomers. However, tautomer **BPP**$_{ac}$ was shown to be <1 kcal/mol less stable than tautomer **BPP**$_{bd}$. All six tautomers gave strongly negative NICS/NICS$_{zz}$ values that are consistent with aromatic systems. In **BPP**$_{bd}$, the NICS results showed that the $\pi$-system for the PAH-unit was essentially disconnected from the porphyrin macrocycle. Ring *a* gave NICS/NICS$_{zz}$ values of +1.83/−2.83, while ring *i* gave larger positive values. This indicates that these rings fall outside of the aromatic pathways. In tautomer **BPP**$_{ac}$,



https://doi.org/10.1021/acs.joc.2c01859
J. Org. Chem. 2022, 87, 16276−16296

ring *a* gives a significantly negative value, although ring *i* still gives positive values. These data suggest that the aromatic pathway runs through the chrysene component but leaves out ring *i*, thereby producing the 34$\pi$ electron pathway highlighted in bold. The conjugation pathway for diprotonated species **BPP**$H_2^{2+}$ gives strongly negative values for rings *a*−*h* but a weaker negative value for ring *i*. This result indicates that the dicationic species favors a 36-atom 34$\pi$ electron pathway as shown in Figure 5. AICD plots for **BPP**$_{ac}$ and **BPP**$H_2^{2+}$ are also consistent with these interpretations (Figure 12). As would be expected, ring fusion results in relatively planar macrocycles for the six free base tautomers and the dicationic species (Table 2).

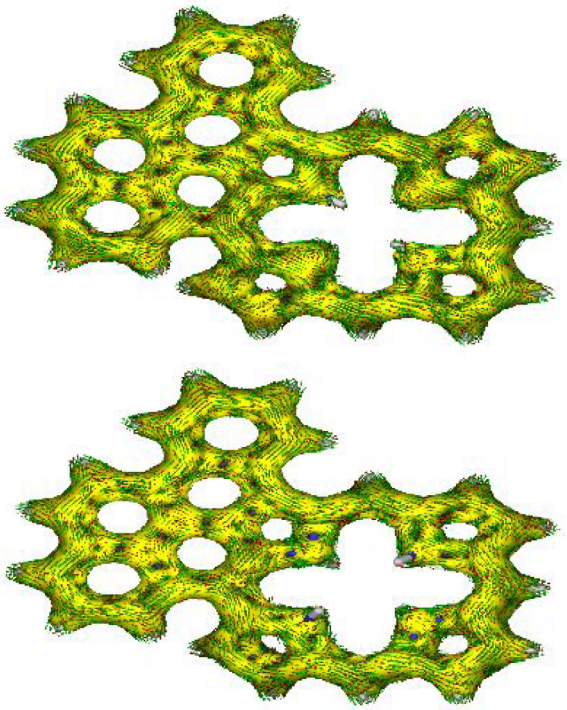

**Figure 12.** AICD plots (isovalues = 0.05) of benzopyrenoporphyrin tautomer **BPP**$_{ac}$ (top) and dication **BPP**$H_2^{2+}$ (bottom).

The effects of ring fusion on porphyrin analogues have also been investigated. Carbaporphyrins have a carbon atom in place of one of the nitrogens in the porphyrin ring system and retain strongly aromatic properties.[30] A route to carbaporphyrins has been developed from carbatripyrrin **36** (Scheme 11), which is easily prepared in three steps from indene.[31] Carbaporphyrins and heterocarbaporphyrins have been prepared from **36**, including the first examples of porphyrin analogues with four different atoms within the macrocyclic cavity.[32] A phenanthrene-fused carbaporphyrin was previously synthesized by this approach,[31] but other examples of PAH-fused carbaporphyrins have not previously been prepared using this methodology. The route provides access to unsubstituted, or parent, porphyrin analogues, but this also results in structures with poor solubility. The possibility that chrysene-ring fusion might improve solubility was appealing. Initially, **36** was reacted with 2,5-pyrroledicarbaldehyde (**37**) in the presence of TFA to give unsubstituted benzocarbaporphyrin **38** (Scheme 11). Although many examples of benzocarbaporphyrins have been reported previously,[30] this is the first time that the parent structure has been synthesized. Benzocarbaporphyrin **38** was sufficiently soluble to give a proton NMR spectrum in $CDCl_3$ (Figure 13), and the *meso*-protons were observed at 10.29 and 10.03 ppm. In addition, the external pyrrolic protons gave rise to two downfield 2H doublets at 9.43 and 9.34 ppm and a 2H singlet at 9.29 ppm. The internal C−H proton gave an upfield singlet at −6.96 ppm, while the NH protons appeared as a broad peak at −3.87 ppm. These results are consistent with a strongly aromatic macrocycle. In the presence of a trace amount of TFA, the corresponding monoprotonated cation **38**$H^+$ also exhibited highly diatropic characteristics and the interior CH was further shielded to give a singlet at −7.29 ppm (Figure 14A). The carbon-13 NMR spectrum for the protonated species gave resonances at 108.8 and 102.0 ppm for the *meso*-carbons, while the internal CH gave a peak at 121.6 ppm. The UV−vis spectrum for **38** gave a Soret band at 418 nm and Q bands at 503, 602, and 660 nm (Figure 15). Addition of TFA led to the formation of a new species, monocation **38**$H^+$, that showed reduced intensity Soret bands and bathochromically shifted Q bands.

Carbatripyrrin **30** was also reacted with chrysopyrrole dialdehyde **19**, pyrenopyrrole dialdehyde **35**,[27] and acenaphthopyrrole dialdehyde **39**[18] to give annulated carbaporphyrins **40**, **41**, and **42**, respectively, in 12−15% yield (Scheme 10). Chrysene-fused benzocarbaporphyrin **40** did not dissolve well in organic solvents, and NMR data could only be obtained for the related monocation **40**$H^+$ (Figure 16) in $CDCl_3$ containing trace amounts of TFA (Figure 14B). As expected, the proton NMR spectrum confirmed that the macrocycle is fully aromatic. The *meso*-protons gave four 1H singlets at 11.74, 11.33, 10.99, and 10.95 ppm, while the internal CH appeared upfield at −6.94 ppm. The UV−vis spectrum of **40** (Figure 17) gave a Soret band at 446 nm and Q bands at 518, 557, 662, and 744 nm (the latter band is comparatively weak). With the exception of the weak long wavelength absorption, the peaks are bathochromically shifted by 15−28 nm; given the increased size of the chromophore, this represents a relatively small change. Spectrophotometric titration with TFA resulted in the formation of monocation **40**$H^+$ which gave a Soret band at 467 nm and weaker absorptions at 562, 601, and 626 nm (Figure 17). Pyrenobenzocarbaporphyrin **41** proved to be particularly insoluble, but a proton NMR spectrum could be obtained in $CDCl_3$ containing trace amounts of TFA (Figure 14C). The *meso*-protons gave two 2H singlets at 11.12 and 10.85 ppm, and the internal CH was observed upfield at −6.44 ppm, confirming the global aromatic character of monoprotonated species **41**$H^+$ (Figure 16). The UV−vis spectrum for **41** was similar to **40**, showing a Soret band at 441 nm and Q bands at 515, 554, 517, and 679 nm (Figure 18). Addition of TFA led to the formation of monocation **41**$H^+$ with a red-shifted Soret band at 460 nm and weaker absorptions at 560 and 625 nm. Acenaphthobenzocarbaporphyrin **42** also proved to have poor solubility in organic solvents. However, the proton NMR spectrum of monoprotonated species **42**$H^+$ (Figure 16) could be obtained in $CDCl_3$ containing trace amounts of TFA at 50 °C (Figure 14D). The *meso*-protons were identified as two 2H singlets at 10.47 and 10.31 ppm, while the interior CH appeared upfield at −6.78 ppm, again confirming the strongly aromatic characteristics of this system. Although it was not possible to obtain a high quality carbon-13 NMR spectrum for **42**$H^+$, some of the carbon resonances could be identified from the HSQC spectrum. The *meso*-carbons were observed at 108.8 and 100.5 ppm, while the interior CH showed up at


https://doi.org/10.1021/acs.joc.2c01859
J. Org. Chem. 2022, 87, 16276−16296

**Scheme 11. Synthesis of Annulated Carbaporphyrins from a Carbatripyrrin**

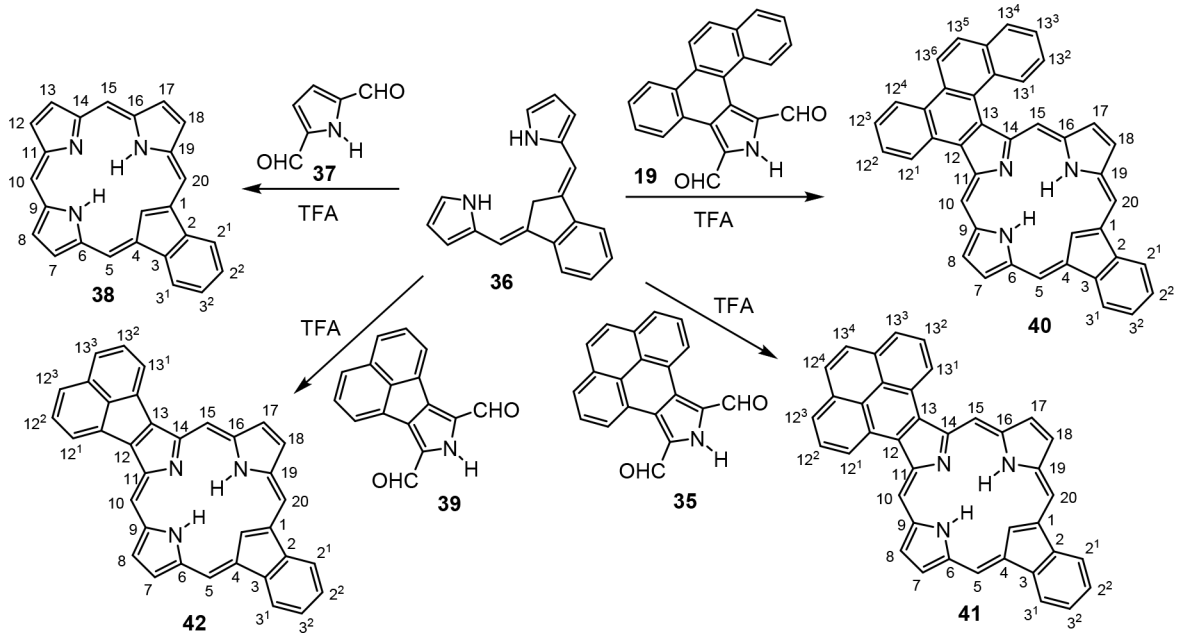


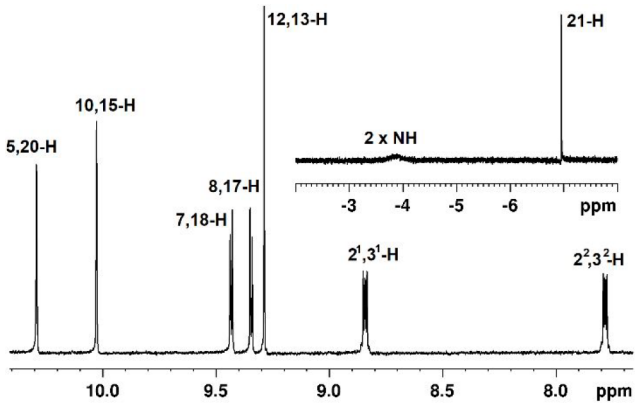


**Figure 13.** Proton NMR spectrum of unsubstituted benzocarbaporphyrin **38** in $CDCl_3$.

121.6 ppm. Fusion of acenaphthylene units to porphyrinoid systems commonly leads to comparatively large bathochromic shifts,[19] but the UV−vis spectrum of **42** (Figure 19) was only slightly red-shifted compared to **40** and **41**. The Soret band for **42** appeared at 450 nm, while the Q bands were seen at 526, 567, and 623 nm. Addition of TFA led to the formation of the related monocation **42**$H^+$, and this gave a Soret band at 470 nm and weaker bands at 567, 614, and 697 nm. The results indicate that **42** is slightly more basic than **38**, **40**, and **41**.

Carbaporphyrins undergo diprotonation in the presence of large excesses of TFA to give dicationic species **38**,**40**−**42**$H_2^{2+}$ (Figure 16).[30] These have modified chromophores and much less intense Soret bands (Figure 20). The Soret band for **38**$H_2^{2+}$ appears at 417 nm and is followed by a series of weaker absorptions. Chrysene-fused carbaporphyrin dication **40**$H_2^{2+}$ gave a broad spectrum, but pyrenocarbaporphyrin dication **41**$H_2^{2+}$ and the related acenaphthylene-fused system **42**$H_2^{2+}$ afforded better resolved spectra with bathochromically shifted Soret bands. The two Soret-like bands for **41**$H_2^{2+}$ appeared at 465 and 504 nm, while **42**$H_2^{2+}$ showed these absorptions at longer wavelength values of 475 and 523 nm. These results indicate that fused pyrene and acenaphthylene units effectively extend the carbaporphyrin chromophore. However, the broad spectrum observed for **40**$H_2^{2+}$ may be caused by the fused chrysene unit disrupting the planarity of the $\pi$-system. Unfortunately, it was not possible to obtain NMR data for the dicationic species.

## CONCLUSIONS

A series of porphyrins with fused chrysene units have been synthesized by a '3 + 1' strategy from a chrysopyrrole dialdehyde and four different tripyrranes. The solubility of chrysoporphyrins is increased compared to related annulated porphyrins, and this was attributed to the chrysene moiety twisting to take on a helical conformation. However, the porphyrin macrocycle retains fully aromatic characteristics. Chrysoporphyrins have two major tautomers, and DFT studies demonstrated that only one of them facilitates aromatic conjugation pathways that pass through the benzenoid unit. Oxidative ring closure with ferric chloride afforded a benzopyrene-fused porphyrin that gave strongly red-shifted absorptions in the visible region. This system also favored two major tautomers, one of which could support a 34$\pi$ electron conjugation pathway. A chrysoporphyrin with an additional fused acenaphthylene ring was also prepared, but this compound had poor solubility and did not show significant long wavelength absorption bands. A series of carbaporphyrins with fused aromatic rings was prepared from a carbatripyrrin, and the observed effects of ring fusion on carbaporphyrins was examined. This work provides access to a novel group of porphyrinoids with extended conjugation and also gives new insights into aromatic conjugation pathways in PAH-fused porphyrinoids.

## EXPERIMENTAL SECTION

Melting points are uncorrected. NMR spectra were recorded using a 400 or 500 MHz NMR spectrometer and were run at 302 K unless otherwise indicated. $^1$H NMR values are reported as chemical shifts $\delta$, relative integral, multiplicity (s, singlet; d, doublet; dd, doublet of doublets, t, triplet; q, quartet; m, multiplet; br, broad peak), and


https://doi.org/10.1021/acs.joc.2c01859
J. Org. Chem. 2022, 87, 16276−16296

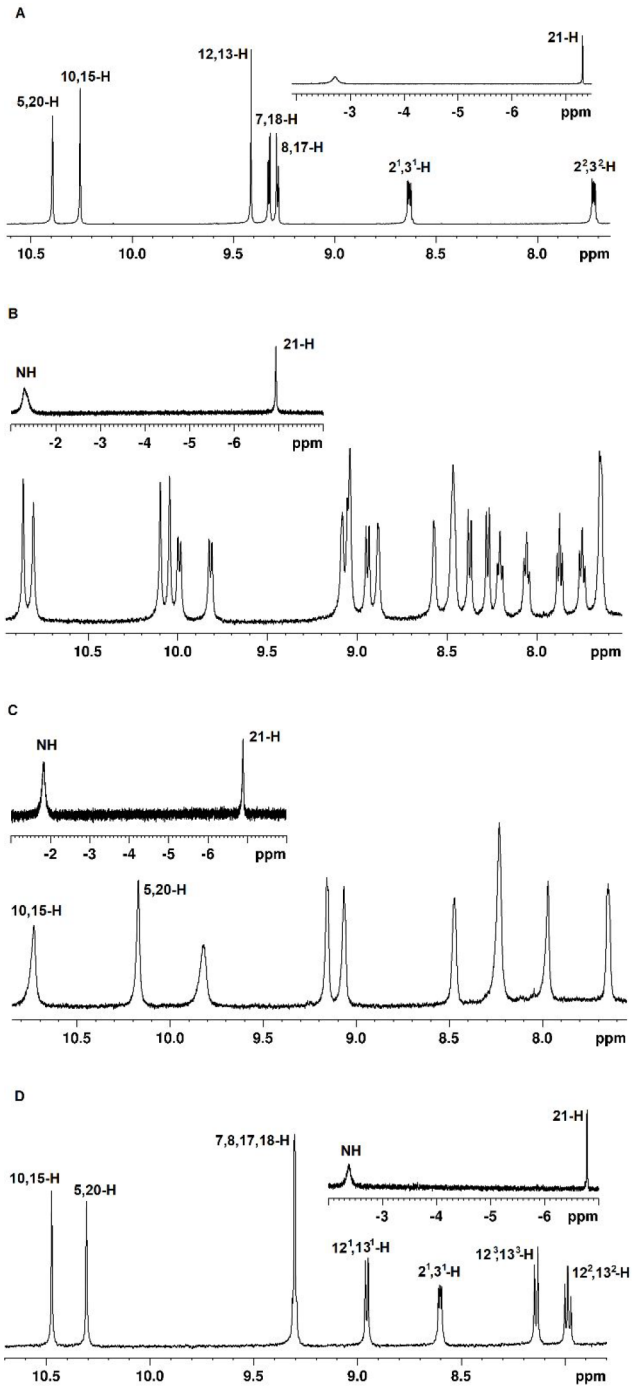


**Figure 14.** Proton NMR spectra of benzocarbaporphyrins **38** (A), **40** (B), **41** (C), and **42** (D) in $CDCl_3$ containing a trace amount of TFA.

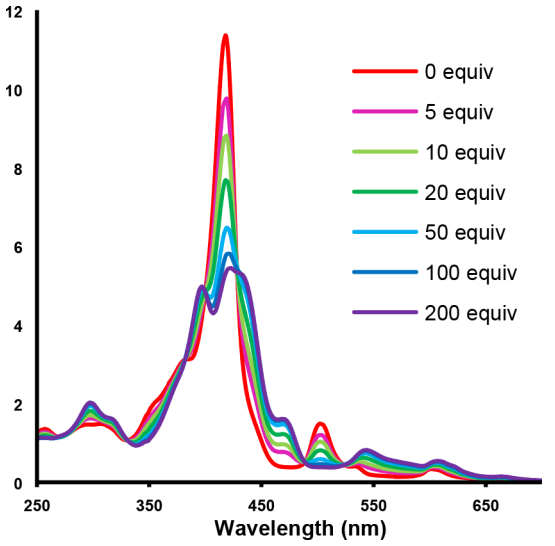


**Figure 15.** UV−vis spectrum of unsubstituted benzocarbaporphyrin **38** in chloroform, and with 5, 10, 20, 50, 100, and 200 equiv of TFA.

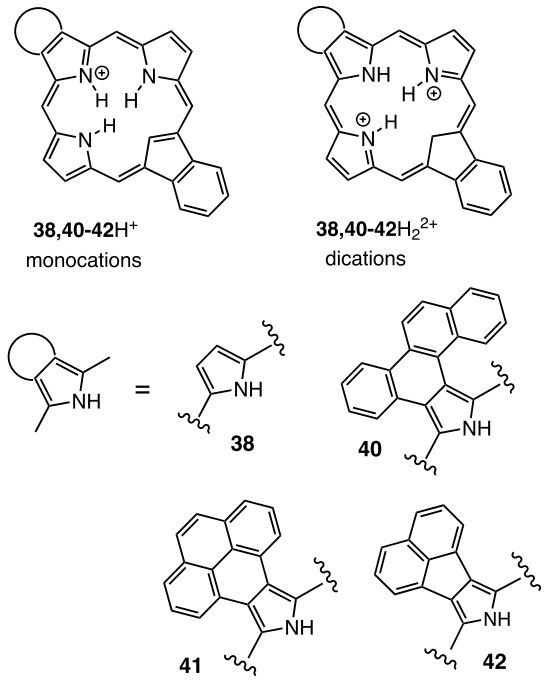


**Figure 16.** Carbaporphyrin dications.

coupling constant ($J$). Chemical shifts are reported in parts per million (ppm) relative to $CDCl_3$ ($^1$H residual $CHCl_3$ singlet $\delta$ 7.26 ppm, $^{13}$C $CDCl_3$ triplet $\delta$ 77.23 ppm) or DMSO-$d_6$ ($^1$H residual DMSO-$d_5$ pentet $\delta$ 2.49 ppm, $^{13}$C DMSO-$d_6$ septet $\delta$ 39.7 ppm), and coupling constants were taken directly from the spectra. NMR assignments were made with the aid of $^1$H−$^1$H COSY, HSQC, DEPT-135, and NOE difference proton NMR spectroscopy. 2D-NMR experiments were performed using standard software. Mass spectral data were acquired using positive-mode electrospray ionization ($ESI^+$) and a high-resolution time-of- flight mass spectrometer.

**Ethyl Chryso[5,6-*c*]pyrrole-1-carboxylate (13).** DBU (1.42 g) was added dropwise to a solution of 6-nitrochrysene (2.56 g, 9.38 mmol) and ethyl isocyanoacetate (1.25 g, 11.0 mmol) in THF (100 mL), and the resulting mixture was stirred under reflux overnight. The mixture was diluted with dichloromethane and washed with water. The organic layer was dried over anhydrous sodium sulfate, filtered, and evaporated under reduced pressure. The residue was loaded onto a silica column with dichloromethane and eluted with 20% hexanes−80% dichloromethane. The product fractions were evaporated, and the residue recrystallized from toluene to give chrysopyrrole **13** (1.50 g, 4.42 mmol, 47%) as white crystals, mp 194.0−195.5 °C. $^1$H NMR (500 MHz, $CDCl_3$): $\delta$ 10.07 (br s, 1H, NH), 8.59 (d, 1H, $J$ = 8.8 Hz, 9-H), 8.59−8.56 (m, 1H, 7-H), 8.42 (d, 1H, $J$ = 8.3 Hz, 13-H), 8.21−8.18 (m, 1H, 4-H), 7.98 (d, 1H, $J$ = 8.8 Hz, 8-H), 7.97 (d, 1H, $J$ = 3.2 Hz, 3-H), 7.94 (d, 1H, $J$ = 8.0 Hz, 10-H), 7.59−7.52 (m, 3H, 5,6,11-H), 7.49−7.46 (m, 1H, 12-H), 4.18 (q, 2H, $J$ = 7.1 Hz, $OCH_2$), 0.89 (t, 3H, $J$ = 7.1 Hz, $CH_2CH_3$). $^{13}$C{$^1$H} NMR (125 MHz, $CDCl_3$): $\delta$ 162.4, 132.6, 130.8, 129.4, 129.3, 129.1 (13-CH), 128.0, 127.4 (8-CH and 5 or 6-CH), 127.2 (10-CH), 126.08 (5 or 6-CH), 126.01 (11-


https://doi.org/10.1021/acs.joc.2c01859
J. Org. Chem. 2022, 87, 16276−16296

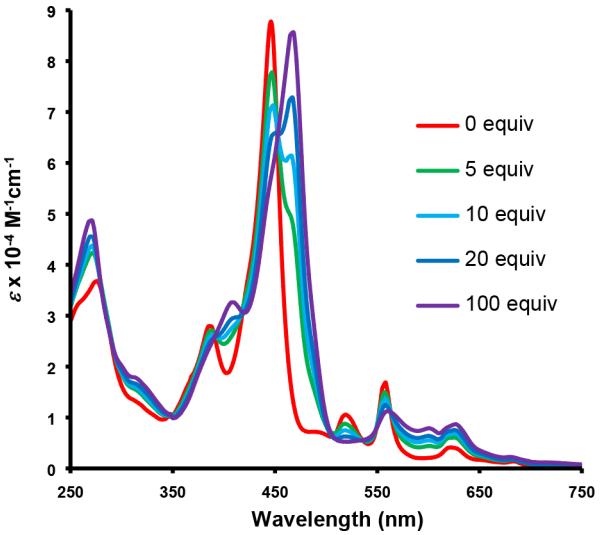


**Figure 17.** UV−vis spectra of chrysobenzocarbaporphyrin **40** in chloroform, and with 0, 5, 10, 20, and 100 equiv of TFA.

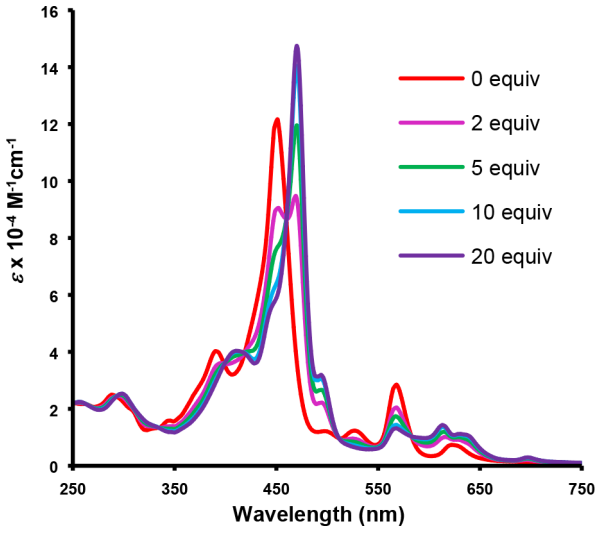


**Figure 19.** UV−vis spectra of acenaphthobenzocarbaporphyrin **42** in chloroform, and with 2, 5, 10, and 20 equiv of TFA.

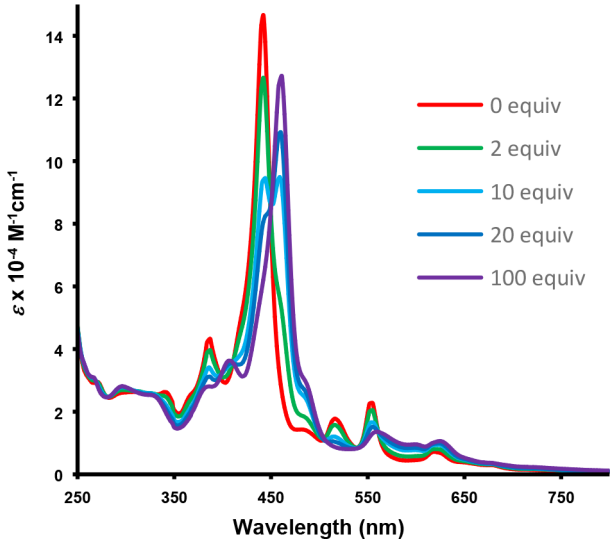


**Figure 18.** UV−vis spectra of pyrenobenzocarbaporphyrin **41** in chloroform, and with 2, 10, 20, and 100 equiv of TFA.

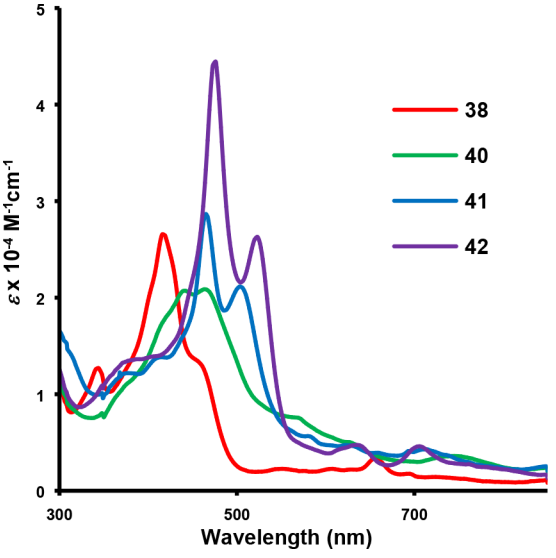


**Figure 20.** UV−vis spectra of **38**, **40**, **41**, and **42** in 50% TFA-$CDCl_3$.

CH), 124.68 (12-CH), 124.63, 124.2 (7-CH), 124.0, 123.0 (4-CH), 121.2 (9-CH), 120.2, 118.9, 115.7 (3-CH), 60.7 ($OCH_2$), 13.8 ($CH_2CH_3$). Anal. Calcd for $C_{23}H_{17}NO_2$: C, 81.40; H, 5.05; N, 4.13. Found: C, 81.60, H, 4.92, N, 3.98.

**Chryso[5,6-*c*]pyrrole (14).** Nitrogen was bubbled through a mixture of ethyl ester **13** (3.21 g, 9.47 mmol), potassium hydroxide (6.6 g), and ethylene glycol (100 mL) for 10 min. The stirred mixture was then heated on an oil bath set to 200 °C for 30 min. The mixture was poured into ice−water (400 mL), and the resulting precipitate was suction filtered and washed with water. After drying in vacuo, the chrysopyrrole (2.45 g, 9.17 mmol, 97%) was obtained as an off-white solid, mp 162−164 °C, dec $^1$H NMR (500 MHz, DMSO-$d_6$): $\delta$ 9.19 (br s, 1H, NH), 8.94 (d, 1H, $J$ = 8.6 Hz), 8.63 (d, 1H, $J$ = 9.0 Hz), 8.60−8.57 (m, 1H), 8.20−8.18 (m, 1H), 8.16 (dd, 1H, $J$ = 2.0, 2.4 Hz), 7.99 (d, 1H, $J$ = 8.0 Hz), 7.91 (d, 1H, $J$ = 8.9 Hz), 7.80 (dd, 1H, $J$ = 1.9, 2.4 Hz, 3-H), 7.68 (ddd, 1H, $J$ = 1.3, 6.8, 7.7 Hz), 7.60 (ddd, 1H, $J$ = 0.9, 6.8, 7.4 Hz), 7.57−7.51 (m, 2H). $^{13}$C{$^1$H} NMR (125 MHz, DMSO-$d_6$): $\delta$ 133.3, 131.1, 129.2, 128.90, 128.88, 127.5, 127.1, 126.6, 126.3, 125.9, 125.7, 125.44, 125.40, 124.4, 123.1, 122.5, 121.7, 118.5, 113.8, 110.1. MS (EI, 70 eV) $m/z$ (%): 267 (100) [$M^+$], 266 (14) [$M^+$ − H], 239 (20) [$M^+$ − H − HCN]. HRMS (ESI) $m/z$: [M + H]$^+$ calcd for $C_{20}H_{14}N$ 268.1121, found 268.1132.

**3-(2-Cyano-2-ethoxycarbonylvinyl)chryso[5,6-*c*]pyrrole (21).** Chrysopyrrole **14** (0.720 g, 2.69 mmol) was taken up in TFA (6 mL) and cooled to <10 °C. Nitrogen was bubbled through the solution for 5 min, and then freshly distilled triethyl orthoformate (6.8 mL) was added rapidly, but dropwise, while maintaining the temperature below 20 °C. The mixture was stirred in the dark for 1 h and poured into water (100 mL). The mixture was basified with 20% aqueous sodium hydroxide and extracted with dichloromethane. The organic solution was dried over anhydrous sodium sulfate, filtered, and evaporated under reduced pressure. The residue was taken up in ethanol (25 mL), ethyl cyanoacetate and 6 drops of pyrrolidine was added, and the stirred mixture was heated under reflux for 3 h. The solution was cooled to room temperature, and the resulting yellow suspension was collected by suction filtration. After drying in vacuo overnight, the cyanovinylpyrrole (820 mg, 2.10 mmol, 78%) was obtained as yellow crystals, mp 243.2−245.0 °C. $^1$H NMR (500 MHz, DMSO-$d_6$): $\delta$ 12.75 (br s, 1H, NH), 8.97 (d, 1H, $J$ = 8.6 Hz), 8.90−8.88 (m, 2H), 8.85 (s, 1H, = CH), 8.81 (d, 1H, $J$ = 9.1 Hz), 8.30−8.28 (m, 1H), 8.12 (d, 1H, $J$ = 7.9 Hz), 8.07 (d, 1H, $J$ = 9.0 Hz), 7.81−7.73 (3H, m), 7.70 (t, 1H, $J$ = 7.4 Hz), 4.36 (q, 2H, $J$ =


https://doi.org/10.1021/acs.joc.2c01859
J. Org. Chem. 2022, 87, 16276−16296

7.1 Hz, $OCH_2$), 1.36 (t, 3H, $J$ = 7.1 Hz, $CH_2CH_3$). $^{13}C\{^1H\}$ NMR (125 MHz, DMSO-$d_6$, 60 °C): $\delta$ 163.3, 141.2, 132.7, 130.8, 129.3, 128.5, 127.7, 127.2, 126.78, 126.75, 126.6, 126.2, 125.9, 124.9, 124.7, 123.5, 121.7, 120.6, 119.8, 117.2, 92.6, 61.6, 14.0. HRMS (ESI) $m/z$: $[M + H]^+$ calcd for $C_{26}H_{19}N_2O_2$ 391.1441, found 391.1438.

**Chryso[5,6-*c*]pyrrole-3-carbaldehyde (20a).** Chrysopyrrole **14** (0.250 g, 0.936 mmol) was reacted with TFA and triethyl orthoformate as described above. The crude product was recrystallized from chloroform−hexanes to give the aldehyde (204 mg, 0.69 mmol, 74%) as an off-white solid, mp 251.5−251.8 °C. $^1H$ NMR (500 MHz, DMSO-$d_6$): $\delta$ 12.0 (v br, 1H, NH), 10.30 (s, 1H, CHO), 9.44−9.38 (br m, 1H, 4-H), 9.05 (d, 1H, $J$ = 8.5 Hz, 13-H), 8.83−8.81 (m, 2H, 1-H and 7-H), 8.79 (d, 1H, $J$ = 9.0 Hz, 8-H), 8.09 (d, 1H, $J$ = 7.8 Hz, 10-H), 8.01 (d, 1H, $J$ = 9.0 Hz, 9-H), 7.77 (t, 1H, $J$ = 7.6 Hz, 12-H), 7.74−7.65 (m, 3H, 5,6,11-H). $^{13}C\{^1H\}$ NMR (125 MHz, DMSO-$d_6$): $\delta$ 179.3, 132.8, 130.1, 129.8, 128.7, 127.4, 127.3, 127.22, 127.18, 127.07, 126.6, 126.43, 126.37, 126.30, 125.3, 124.4, 124.0, 122.1, 120.8. HRMS (ESI) $m/z$: $[M + H]^+$ calcd for $C_{21}H_{14}NO$ 296.1070, found 296.1073.

**Chryso[5,6-*c*]pyrrole-1,3-dicarbaldehyde (19).** Stirred DMF (1.0 mL) was cooled in an ice-salt bath, and phosphorus oxychloride was added dropwise while maintaining the temperature between 10 and 20 °C. The ice-salt bath was removed, and the mixture was kept at room temperature for 15 min. The resulting Vilsmeier complex was dissolved in 6 mL of dichloromethane, and the mixture was cooled to 0−2 °C with the aid of a salt-ice bath. A solution of cyanovinylchrysopyrrole **21** (820 mg, 2.10 mmol) in dichloromethane was added over 15 min, and the mixture was then refluxed for 15 min. The mixture was cooled to room temperature, a solution of sodium acetate trihydrate (10.1 g) in water (14 mL) was added, and the mixture was stirred under reflux for an additional 15 min. After cooling the reaction mixture, the two layers were separated, and the aqueous phase was extracted with chloroform. The combined organic solutions were washed with saturated sodium carbonate and dried over sodium sulfate. The solvent was removed on a rotary evaporator, and the residue was heated under reflux with 3 M aqueous sodium hydroxide (40 mL) for 30 min. The product precipitated from solution and was collected by suction filtration. After drying in vacuo, the dialdehyde (675 mg, 2.09 mmol, quantitative) was obtained as a saffron yellow solid, mp 225.3−225.8 °C. $^1H$ NMR (500 MHz, DMSO-$d_6$): $\delta$ 14.12 (br s, 1H, NH), 10.42 (s, 1H, 3-CHO), 10.30 (s, 1H, 1-CHO), 9.52−9.50 (m, 1H, 4-H), 8.81−8.77 (m, 2H, 7,8-H), 8.74−8.72 (m, 1H, 13-H), 8.12 (d, 1H, $J$ = 8.8 Hz, 9-H), 8.09−8.07 (m, 1H, 10-H), 7.75−7.69 (m, 2H, 5,6-H), 7.65−7.60 (m, 2H, 11,12-H). $^{13}C\{^1H\}$ NMR (125 MHz, DMSO-$d_6$, 60 °C): $\delta$ 182.3, 180.5, 132.6, 130.4, 130.06, 129.99, 129.8, 128.1, 127.53, 127.50, 127.2, 127.0, 126.9, 126.7, 126.5, 126.2, 124.4, 123.9, 122.6, 122.3, 121.3. HRMS (ESI) $m/z$: $[M + H]^+$ calcd for $C_{22}H_{14}NO_2$ 324.1019, found 324.1023.

**Ethyl 4-Hexyl-3,5-dimethylpyrrole-2-carboxylate (32).** Iodohexane (70.50 g, 0.332 mol) was added dropwise to a solution of potassium carbonate (27.96 g, 0.202 mol) and 2,4-pentadione (35 mL) in acetone (42 mL) and refluxed for 4 days with vigorous stirring. The mixture was filtered and washed with acetone, and the solvent was removed under reduced pressure. The residue was distilled under reduced pressure (water aspirator) to afford 3-hexyl-2,4-pentadione (45.95 g, 0.249 mol, 75%) as a colorless oil, bp 130−140 °C at 20 mmHg (lit. bp[33] 111−113 °C at 15 mmHg). A mixture of diethyl aminomalonate (9.45 g, 54.0 mmol) and 3-hexyl-2,4-pentanedione (10.00 g, 54.3 mmol) was added over several minutes to gently boiling acetic acid (20 mL), and the resulting solution was stirred under reflux for 1 h. The mixture was cooled to 70 °C, poured into ice/water (~250 mL), and allowed to stand overnight. The precipitate was suction filtered, washed with 60% ethanol−water, and recrystallized from ethanol to afford ethyl 4-hexyl-3,5-dimethylpyrrole-2-carboxylate (6.08 g, 24.2 mmol, 45%) as white crystals, mp 63.6−64.0 °C (lit mp[34] 59 °C; 62−63 °C[35]). $^1H$ NMR (500 MHz, $CDCl_3$): $\delta$ 8.48 (br s, 1H, NH), 4.29 (q, 2H, $J$ = 7.1 Hz, $OCH_2$), 2.34 (t, 2H, $J$ = 7.5 Hz), pyrrole-$CH_2$), 2.25 (s, 3H), 2.19 (s, 3H) (2 × pyrrole-$CH_3$), 1.44−1.38 (m, 2H, pyrrole-$CH_2CH_2$), 1.34 (t, 3H, $J$ = 7.1 Hz, $OCH_2CH_3$), 1.31−1.27 (m, 6H, $CH_2(CH_2)_3CH_3$), 0.88 (t, 3H, $J$ = 6.8 Hz, $(CH_2)_5CH_3$). $^{13}C\{^1H\}$ NMR (125 MHz, $CDCl_3$): $\delta$ 161.9, 129.4, 127.3, 122.7, 116.9, 50.7, 32.0, 31.0, 29.4, 24.3, 22.9, 14.8, 14.3, 11.8, 10.8.

**Benzyl 4-Hexyl-3,5-dimethylpyrrole-2-carboxylate (33).** A sodium benzyloxide solution was prepared by reacting sodium metal (0.20 g, 8.7 mmol) with benzyl alcohol (10 mL). A small amount of the sodium benzyloxide solution was added to ethyl ester **32** (17.204 g, 0.0684 mol) and benzyl alcohol (25 mL) in an Erlenmeyer flask equipped with a magnetic stir bar, and the mixture was gradually heated with the aid of an oil bath from room temperature to 230 °C over a period of 90 min while adding the majority of the sodium benzyloxide in small portions. The temperature of the vapors approximately 4 cm above the solution was monitored with a thermometer, and when the vapor temperature reached 175 °C, a final portion of the sodium benzyloxide solution (ca. 1 mL) was added. The mixture was stirred for a further 5 min, and the hot solution was poured into a chilled mixture of methanol (80 mL), water (50 mL), and acetic acid (1 mL). The resulting precipitate was suction filtered, recrystallized from 95% ethanol, and dried in a vacuum desiccator to afford the benzyl ester (18.318 g, 0.0585 mol, 85%) as a white solid, mp 63.4−63.7 °C. $^1H$ NMR (500 MHz, $CDCl_3$): $\delta$ 8.46 (br s, 1H, NH), 7.43−7.41 (m, 2H, 2 × $o$-H), 7.36 (t, 2H, $J$ = 7.5 Hz, $m$-H), 7.33−7.29 (m, 1H, $p$-H), 5.30 (s, 2H, $CH_2Ph$), 2.35 (t, 2H, $J$ = 7.6 Hz, pyrrole-$CH_2$), 2.29 (s, 3H), 2.18 (s, 3H) (2 × pyrrole-$CH_3$), 1.46−1.40 (m, 2H, pyrrole-$CH_2CH_2$), 1.33−1.29 (m, 6H, $(CH_2)_3CH_3$), 0.90 (t, 3H, $J$ = 6.8 Hz, $(CH_2)_5CH_3$). $^{13}C\{^1H\}$ NMR (125 MHz, $CDCl_3$): $\delta$ 161.5, 129.8, 128.7, 128.3, 128.2, 128.0, 123.0, 116.8, 65.6, 32.0, 31.0, 29.4, 24.3, 22.9, 14.2, 11,7, 10.9. HRMS (ESI) $m/z$: $[M + H]^+$ calcd for $C_{20}H_{28}NO_2$ 314.2115, found 314.2102.

**Benzyl 5-Acetoxymethyl-4-hexyl-3-methylpyrrole-2-carboxylate (24c).** Benzyl 4-hexyl-3,5-dimethylpyrrole-2-carboxylate (3.266 g, 10.4 mmol) was dissolved in acetic acid (80 mL) and acetic anhydride (4 mL), lead tetraacetate (4.50 g, 10.0 mmol) was added, and the mixture stirred at room temperature overnight. The mixture was poured into ice−water, and the precipitate was collected by suction filtration. Recrystallization from chloroform−hexanes gave the acetoxymethylpyrrole (2.435 g, 6.56 mmol, 65%) as a white solid, mp 96.1−96.6 °C. $^1H$ NMR (500 MHz, $CDCl_3$): $\delta$ 8.98 (br s, 1H, NH), 7.43−7.41 (m, 2H, 2 × $o$-H), 7.37 (t, 2H, $J$ = 7.4 Hz, 2 × $m$-H), 7.34−7.31 (m, 1H, $p$-H), 5.31 (s, 2H, $OCH_2Ph$), 5.01 (s, 2H, $CH_2OAc$), 2.42 (t, 2H, $J$ = 7.6 Hz, pyrrole-$CH_2CH_2$), 2.28 (s, 3H, 3-Me), 2.06 (s, 3H, $OC(O)CH_3$), 1.45−1.40 (m, 2H, pyrrole-$CH_2CH_2$), 1.38−1.26 (m, 6H, $CH_2(CH_2)_3CH_3$), 0.88 (t, 3H, $J$ = 6.7 Hz, $(CH_2)_5CH_3$). $^{13}C\{^1H\}$ NMR (125 MHz, $CDCl_3$): $\delta$ 171.7, 161.3, 136.5, 128.8 (2 × $m$-CH), 128.36 (2 × $o$-CH), 128.32 ($p$-CH), 127.4, 127.0, 125.7, 119.1, 65.9 ($OCH_2Ph$), 57.2 ($CH_2OAc$), 31.9, 31.5 (4-$CH_2CH_2$), 29.3, 24.1 (4-$CH_2$), 22.8, 21.1 ($OC(O)CH_3$), 14.3 ($CH_2CH_3$), 10.7 (3-Me). HRMS (ESI) $m/z$: $[M + H]^+$ calcd for $C_{22}H_{30}NO_4$ 372.2169, found 372.2155.

**2,5-Bis(5-benzyloxycarbonyl-3-hexyl-4-methyl-2-pyrrolylmethyl)-3,4-diethylpyrrole (25c).** Benzyl 5-acetoxymethyl-4-hexyl-3-methylpyrrole-2-carboxylate (0.911 g, 2.45 mmol) and 3,4-diethylpyrrole[36] (0.151 g, 1.23 mmol) were dissolved in ethanol (9 mL) and acetic acid (0.5 mL) and refluxed with stirring under nitrogen overnight. The mixture was cooled in ice, and the precipitate was collected by suction filtration and dried in vacuo to afford the tripyrrane (660 mg, 0.885 mmol, 72%) as a white solid, mp 153.0−156.4 °C. $^1H$ NMR (500 MHz, $CDCl_3$): $\delta$ 10.58 (br s, 2H, 2 × NH), 8.37 (br s, 1H, NH), 7.27−7.21 (m, 6H, $m$- and $p$-H), 7.08−7.05 (d, 4H, 4 × $o$-H), 4.57 (br s, 4H, 2 × $CH_2Ph$), 3.58 (s, 4H, 2 × bridge-$CH_2$), 2.47 (q, 4H, $J$ = 7.5 Hz, 2 × $CH_2CH_3$), 2.28 (t, 4H, 2 × pyrrole-$CH_2CH_2$), 2.23 (s, 6H, 2 × pyrrole-$CH_3$), 1.34−1.19 (m, 16H, $2(CH_2)_4CH_3$), 1.13 (t, 6H, $J$ = 7.5 Hz, 2 × pyrrole-$CH_2CH_3$), 0.86 (6H, t, $J$ = 6.9 Hz, $2(CH_2)_5CH_3$). $^{13}C\{^1H\}$ NMR (125 MHz, $CDCl_3$): $\delta$ 162.3, 137.2, 132.5, 128.5, 127.7, 127.5, 127.4, 122.4, 120.4, 117.5, 65.6, 32.0, 31.3, 29.6, 24.3, 22.92, 22.86, 18.0, 16.8, 14.2, 11.1. HRMS (ESI) $m/z$: $[M + H]^+$ calcd for $C_{48}H_{64}N_3O_4$ 746.4891, found 746.4872.

**2,5-Bis(5-benzyloxycarbonyl-3,4-dimethyl-2-pyrrolylmethyl)-3,4-diethylpyrrole (25b).** Benzyl 5-acetoxymethyl-3,4-dimethyl-


https://doi.org/10.1021/acs.joc.2c01859
J. Org. Chem. 2022, 87, 16276−16296

pyrrole-2-carboxylate (2.45 g, 8.14 mmol)[37] and 3,4-diethylpyrrole[36] (0.50 g, 4.06 mmol) were dissolved in 2-propanol (16 mL) and acetic acid (1 mL) and refluxed with stirring under nitrogen overnight. The mixture was cooled in ice, and the precipitate was collected by suction filtration and dried under vacuum to afford the tripyrrane (1.556 g, 2.57 mmol, 63%) as a white solid, mp 195−199 °C, dec $^1$H NMR (500 MHz, $CDCl_3$): $\delta$ 10.96 (br s, 2H, 2 × NH), 8.73 (br s, 1H, NH), 7.27−7.21 (m, 6H, *m*- and *p*-H), 7.02 (d, 4H, $J$ = 7.2 Hz, 4 × *o*-H), 4.41 (br s, 4H, 2 × $CH_2$Ph), 3.54 (br s, 4H, 2 × bridge-$CH_2$), 2.35 (q, 4H, $J$ = 7.5 Hz, 2 × $CH_2CH_3$), 2.25 (s, 6H, 2 × pyrrole-4-Me), 2.00 (s, 6H, 2 × pyrrole-3-Me), 0.97 (t, 6H, $J$ = 7.5 Hz, 2 × $CH_2CH_3$). $^{13}$C{$^1$H} NMR (125 MHz, $CDCl_3$): $\delta$ 162.8, 137.2, 133.0, 128.3 (4 × *m*-CH), 127.5 (2 × *p*-CH), 127.0 (4 × *o*-CH), 123.3, 123.0, 117.4, 112.7, 65.5 (2 × $OCH_2$), 22.4 (2 × bridge-$CH_2$), 17.4 (2 × $CH_2CH_3$), 15.9 (2 × $CH_2CH_3$), 11.2 (2 × pyrrole 4-Me, 9.5 (2 × pyrrole 3-Me). HRMS (ESI) $m/z$: M$^+$ calcd for $C_{38}H_{43}N_3O_4$ 605.3254, found 605.3259.

**Standard Procedure for the Preparation of Tripyrrane Dicarboxylic Acids 23.** In a hydrogenation vessel, dibenzyl tripyrrane **25c** (503 mg, 0.674 mmol) was taken up in acetone (100 mL), methanol (25 mL), and triethylamine (10 drops) and subsequently purged with nitrogen. Following the addition of approximately 70 mg of 10% Pd/C, the vessel was shaken under 40 psi of $H_2$ for 6−8 h. After removing the catalyst by suction filtration, the solvent was evaporated under reduced pressure. The residue was dissolved in 5% aqueous ammonia (ca.15 mL) and ethanol (5−8 mL; this aids the solubility in this case, but ethanol was not required in the preparation of other tripyrrane dicarboxylic acids), and the mixture was cooled in an ice-salt bath to 0−5 °C. The solution was neutralized with acetic acid while maintaining the temperature below 5 °C. After allowing the flask to stand for approximately 30 min to ensure complete precipitation, the product was collected by suction filtration and following vacuum desiccation overnight, tripyrrane dicarboxylic acid **23c** (363.5 mg, 0.642 mmol, 97%) was isolated as an unstable pale pink powder that was used without further purification.

**1,3-(5-*tert*-Butoxycarbonyl-3-ethyl-4-methyl-2-pyrrolylmethyl)chrysopyrrole[5,6-*c*]pyrrole (16a).** Chrysopyrrole **14** (100 mg, 0.374 mmol) and acetoxymethylpyrrole **15a**[37] (211 mg, 0.75 mmol) in acetic acid (0.5 mL) and ethanol (5 mL) were refluxed with stirring under nitrogen for 16 h. The mixture was cooled, and the precipitate was suction filtered and washed with cold ethanol to give chrysotripyrrane **16a** (238 mg, 0.335 mmol, 90%) as an off-white solid, mp 140.7−142.0 °C. $^1$H NMR (500 MHz, $CDCl_3$): $\delta$ 8.57 (br s, 1H, NH), 8.54 (d, 1H, $J$ = 9.0 Hz), 8.53−8.51 (m, 1H), 8.33−8.30 (m, 1H), 8.10 (br s, 1H, NH), 8.05−8.02 (m, 1H), 7.96−7.94 (m, 2H), 7.90 (d, 1H, $J$ = 9.0 Hz), 7.54−7.49 (m, 4H), 4.46 (s, 2H), 4.15 (s, 2H), 2.28 (s, 3H), 2.22 (s, 3H), 2.28−2.23 (m, 4H), 1.54 (s, 9H), 1.47 (s, 9H), 0.90−0.85 (m, 6H). $^{13}$C{$^1$H} NMR (125 MHz, $CDCl_3$): $\delta$ 161.2, 160.9, 133.4, 130.0, 129.9, 129.4, 128.5, 128.3, 127.74, 127.66, 127.1, 127.0, 126.6, 126.4, 126.3, 125.9, 125.5, 125.03, 124.96, 124.8, 124.7, 124.2, 123.7, 121.8, 120.9, 120.8, 119.9, 119.6, 117.4, 117.1, 80.6, 80.5, 28.74, 28.68, 27.9, 26.6, 17.2, 15.6, 15.4, 10.7, 10.6. HRMS (ESI) $m/z$: M$^+$ calcd for $C_{46}H_{51}N_3O_4$ 709.3880, found 709.3899.

**1,3-(5-*tert*-Butoxycarbonyl-3,4-dimethyl-2-pyrrolylmethyl)-chrysopyrrole[5,6-*c*]pyrrole (16b).** Chrysopyrrole **14** (100 mg, 0.374 mmol) and acetoxymethylpyrrole **15b**[38] (200 mg, 0.374 mmol) in acetic acid (0.5 mL) and ethanol (5 mL) were refluxed with stirring under nitrogen for 16 h. The mixture was cooled, and the precipitate was suction filtered and washed with cold ethanol to give chrysotripyrrane **16b** (158.4 mg, 0.233 mmol, 62%) as a white solid, mp 216−217 °C, dec $^1$H NMR (500 MHz, $CDCl_3$): $\delta$ 8.58 (br s, 1H, NH), 8.54 (d, 1H, $J$ = 8.9 Hz), 8.52−8.50 (m, 1H), 8.33−8.31 (m, 1H), 8.16 (br s, 1H, NH), 8.03−8.00 (m, 2H), 7.96−7.93 (m, 1H), 7.90 (d, 1H, $J$ = 8.9 Hz), 7.54−7.49 (m, 4H), 4.45 (s, 2H), 4.15 (s, 2H), 2.27 (s, 3H), 2.20 (s, 3H), 1.80 (s, 3H), 1.77 (s, 3H), 1.53 (s, 9H), 1.48 (s, 9H). $^{13}$C{$^1$H} NMR (125 MHz, $CDCl_3$): $\delta$ 161.3, 161.0, 133.4, 130.0, 129.9, 129.4, 128.6, 127.73, 127.66, 127.61, 127.1, 127.02, 127.01, 126.6, 125.9, 125.5, 125.0, 124.7, 124.2, 123.7, 121.8, 120.8, 120.7, 119.6, 119.2, 118.2, 117.8, 117.4, 117.1, 80.7, 80.5, 28.73, 28.69, 28.2, 26.7, 10.8, 10.7, 8.7. HRMS (ESI) $m/z$: M$^+$ calcd for $C_{44}H_{47}N_3O_4$ 681.3567, found 681.3574.

**8,12,13,17-Tetraethyl-7,18-dimethylchryso[5,6-*b*]porphyrin (11a).** Tripyrrane dicarboxylic acid **23a**[23,24] (80 mg, 0.176 mmol) was stirred with TFA (1 mL) under nitrogen for 1 min. The mixture was diluted with dichloromethane (15 mL), and chrysopyrrole dialdehyde **19** (57.0 mg, 0.176 mg) was added. Stirring under nitrogen was continued for 2 h. The solution was neutralized by the dropwise addition of triethylamine, DDQ (40 mg, 0.176 mmol) was added, and the mixture was stirred for a further 1 h. The solution was washed with water and evaporated under reduced pressure. The residue was purified on a grade 3 alumina column eluting with dichloromethane. Recrystallization from chloroform−methanol afforded the chrysoporphyrin (51.3 mg, 0.079 mmol, 45%) as purple crystals, mp >300 °C. UV−vis ($CHCl_3$; 1.068 × 10$^{-5}$ M): $\lambda_{max}$/nm (log $\varepsilon$) 277 (4.59), 333 (4.39), 404 (sh, 4.98), 425 (5.21), 493 (sh, 3.52), 525 (3.91), 563 (4.57), 582 (4.26), 638 (3.62). UV−vis (100 equiv TFA-$CHCl_3$; 1.068 × 10$^{-5}$ M): $\lambda_{max}$/nm (log $\varepsilon$) 272 (4.76), 422 (5.12), 574 (4.16), 626 (4.44). UV−vis (5% TFA-$CHCl_3$; 1.068 × 10$^{-5}$ M): $\lambda_{max}$/nm (log $\varepsilon$) 412 (5.11), 576 (4.09), 629 (4.36). $^1$H NMR (500 MHz, $CDCl_3$, 55 °C): $\delta$ 11.27 (s, 1H, 5-H), 11.11 (s, 1H, 20-H), 10.13 (d, 1H, $J$ = 8.2 Hz), 10.04 (s, 1H, 10- or 15-H), 10.01 (d, 1H, $J$ = 8.8 Hz, 3$^1$-H), 10.00 (s, 1H, 10- or 15-H), 9.07 (d, 1H, $J$ = 8.3 Hz, 2$^4$-H), 9.00 (d, 1H, $J$ = 8.8 Hz, 3$^6$-H), 8.25 (d, 1H, $J$ = 8.8 Hz, 3$^5$-H), 8.23 (d, 1H, $J$ = 8.0 Hz, 3$^4$-H), 8.11 (t, 1H, $J$ = 7.5 Hz, 2$^2$-H), 7.90 (t, 1H, $J$ = 7.5 Hz, 2$^3$-H), 7.80 (t, 1H, $J$ = 7.4 Hz, 3$^3$-H), 7.59 (t, 1H, $J$ = 7.5 Hz, 3$^2$-H), 4.19 (q, 2H, $J$ = 7.7 Hz), 4.11 (q, 2H, $J$ = 7.7 Hz), 4.05−4.00 (m, 4H) (4 × $CH_2CH_3$), 3.82 (s, 3H, 18-Me), 3.39 (s, 3H, 7-Me), 1.94−1.86 (m, 12H, 4 × $CH_2CH_3$), −3.24 (br s, 2H, 2 × NH). $^1$H NMR (500 MHz, TFA-$CDCl_3$): $\delta$ 11.78 (s, 1H, 5-H), 11.38 (s, 1H, 20-H), 10.58 (s, 1H), 10.54 (s, 1H) (10,15-H), 9.97 (d, 1H, $J$ = 8.0 Hz, 2$^1$-H), 9.49 (d, 1H, $J$ = 8.4 Hz, 3$^1$-H), 9.27 (d, 1H, $J$ = 8.3 Hz, 2$^4$-H), 9.15 (d, 1H, $J$ = 8.9 Hz, 3$^6$-H), 8.52 (d, 1H, $J$ = 8.8 Hz, 3$^5$-H), 8.38 (t, 1H, $J$ = 7.5 Hz, 2$^2$-H), 8.34 (d, 1H, $J$ = 8.0 Hz, 3$^4$-H), 8.26 (t, 1H, $J$ = 7.5 Hz, 2$^3$-H), 7.91 (t, 1H, $J$ = 7.4 Hz, 3$^3$-H), 7.69 (t, 1H, $J$ = 7.5 Hz, 3$^2$-H), 4.18−4.04 (m, 8H, 2 × $CH_2CH_3$), 3.66 (s, 3H, 18-Me), 3.30 (s, 3H, 7-Me), 1.80−1.70 (m, 9H), 1.64 (t, 3H, $J$ = 7.7 Hz) (2 × $CH_2CH_3$), −2.53 (s, 1H), −2.63 (s, 1H), −3.65 (br s, 1H), −3.71 (s, 1H) (4 × NH). $^{13}$C{$^1$H} NMR (125 MHz, $CDCl_3$): $\delta$ 152.9, 152.7, 148.8, 148.6, 144.49, 144.46, 140.0, 139.7, 138.0, 137.8, 137.4, 137.2, 137.1, 136.6, 134.0, 133.6, 132.1, 130.7, 130.5, 129.93, 129.89, 127.98, 127.96, 127.6, 127.3, 126.9, 126.4, 126.3, 125.1, 124.9, 122.1, 100.8, 100.2, 96.9, 96.7, 20.1, 20.0, 18.6, 17.63, 17.55, 11.8, 11.3. $^{13}$C{$^1$H} NMR (125 MHz, TFA-$CDCl_3$): $\delta$ 143.5, 143.1, 142.8, 142.76, 142.72, 142.63, 142.61, 142.5, 142.2, 141.0, 138.9, 137.5, 137.1, 136.4, 134.0, 133.2, 131.8, 131.5, 130.35, 130.31, 129.3, 129.2, 128.6, 128.48, 128.41, 128.36, 128.1, 126.9, 126.2, 125.4, 125.3, 121.6, 100.9, 100.2, 97.7, 97.5, 20.32, 20.24, 20.18, 20.17, 17.64, 17.61, 16.68, 16.60, 12.1, 11.5. HRMS (ESI) $m/z$: [M + H]$^+$ calcd for $C_{46}H_{43}N_4$ 651.3488, found 651.3481.

**[8,12,13,17-Tetraethyl-7,18-dimethylchryso[5,6-*b*]-porphyrinato]nickel(II) (26a).** Chrysoporphyrin **11a** (10.0 mg, 0.0154 mmol) was dissolved in chloroform (10 mL). A saturated solution of nickel(II) acetate in methanol (5 mL) was added, and the mixture was heated under reflux overnight. The solution was diluted with chloroform and washed with water, and the solvent was removed on a rotary evaporator. The residue was purified on a grade 3 alumina column, eluting with dichloromethane, and recrystallized from chloroform−methanol to give the nickel complex (9.7 mg, 0.137 mmol, 89%) as a purple solid, mp >300 °C. UV−vis ($CHCl_3$; 1.710 × 10$^{-5}$ M): $\lambda_{max}$/nm (log $\varepsilon$) 419 (5.11), 540 (3.94), 586 (4.60). $^1$H NMR (500 MHz, $CDCl_3$): $\delta$ 10.56 (s, 1H, 5-H), 10.55 (s, 1H, 20-H), 9.69 (d, 1H, $J$ = 8.2 Hz, 2$^1$-H), 9.64 (s, 1H), 9.58 (s, 1H) (10,15-H), 9.24 (d, 1H, $J$ = 8.6 Hz, 3$^1$-H), 9.08 (d, 1H, $J$ = 8.4 Hz, 2$^4$-H), 9.02 (d, 1H, $J$ = 9.0 Hz, 3$^6$-H), 8.25 (d, 1H, $J$ = 8.9 Hz, 3$^5$-H), 8.15 (d, 1H, $J$ = 8.0 Hz, 3$^4$-H), 8.03 (t, 1H, $J$ = 7.6 Hz, 2$^2$-H), 7.87 (t, 1H, $J$ = 7.6 Hz, 2$^3$-H), 7.65 (t, 1H, $J$ = 7.4 Hz, 3$^3$-H), 7.28 (t, 1H, $J$ = 7.7 Hz, 3$^2$-H), 3.94−3.88 (m, 6H, 3 × $CH_2CH_3$), 3.79 (q, 2H, $J$ = 7.6 Hz, 8-$CH_2$), 3.54 (s, 3H, 18-Me), 3.06 (s, 3H, 7-Me), 1.86−1.80 (m, 9H, 3 × $CH_2CH_3$), 1.73 (t, 3H, $J$ = 7.6 Hz, 8- $CH_2CH_3$). $^{13}$C{$^1$H} NMR (125


https://doi.org/10.1021/acs.joc.2c01859
J. Org. Chem. 2022, 87, 16276−16296

MHz, $CDCl_3$): δ 143.9, 143.6, 143.22, 143.21, 141.6, 141.2, 140.98, 140.93, 140.7, 140.6, 137.8, 137.1, 136.9, 136.6, 135.7, 135.4, 133.5, 131.3, 129.9, 129.28, 129.18 ($3^1$-CH), 128.8, 128.2 ($2^2$-CH), 128.1 ($3^4$-CH), 127.9 ($3^5$-CH), 127.2 ($3^3$-CH), 126.4 ($2^3$-CH), 126.3 ($2^1$-CH), 125.2, 125.05 ($2^4$-CH), 125.01 ($3^2$-CH), 122.1 ($3^6$-CH), 99.8 (5-CH), 99.3 (20-CH), 97.3, 97.0 (10,15-CH), 20.0, 19.90, 19.88, 18.47, 18.46, 17.7, 17.6, 11.8 (18-Me), 11.2 (7-Me). HRMS (ESI) *m/z*: $M^+$ calcd for $C_{46}H_{40}N_4Ni$ 706.2606, found 706.2604.

**[8,12,13,17-Tetraethyl-7,18-dimethylchryso[5,6-*b*]-porphyrinato]copper(II) (26b).** Chrysoporphyrin **11a** (10.0 mg, 0.0154 mmol) was dissolved in chloroform (10 mL), a saturated solution of copper(II) acetate in methanol (5 mL) was added, and the mixture was heated under reflux for 2 h. The solution was diluted with chloroform, washed with water, and the solvent was removed on a rotary evaporator. The residue was purified on a grade 3 alumina column, eluting with dichloromethane, and recrystallized from chloroform−methanol to give the copper complex (9.1 mg, 0.0128 mmol, 83%) as a dark solid, mp >300 °C. UV−vis ($CHCl_3$; 1.546 × $10^{-5}$ M): $\lambda_{max}$/nm (log ε) 419 (5.27), 546 (4.01), 593 (4.61). HRMS (ESI) *m/z*: $M^+$ calcd for $C_{46}H_{40}N_4Cu$ 711.2549, found 711.2548.

**[8,12,13,17-Tetraethyl-7,18-dimethylchryso[5,6-*b*]-porphyrinato]zinc(II) (26c).** Chrysoporphyrin **11a** (10.0 mg, 0.0154 mmol) was dissolved in chloroform (10 mL). A saturated solution of zinc acetate in methanol (5 mL) was added, and the mixture was heated under reflux for 90 min. The solution was diluted with chloroform, washed with water, and the solvent was removed on a rotary evaporator. The residue was recrystallized from chloroform−methanol to give the zinc complex (10.5 mg, 0.0147 mmol, 96%) as a dark green solid, mp >300 °C. UV−vis (1% pyrrolidine-$CHCl_3$; 1.627 × $10^{-5}$ M): $\lambda_{max}$/nm (log ε) 416 (sh, 4.72), 440 (5.24), 563 (4.16), 608 (4.56), 681 (3.85). $^1$H NMR (500 MHz, DMSO-$d_6$): δ 11.14 (s, 1H), 11.12 (s, 1H), 10.33 (d, 1H, *J* = 8.3 Hz), 10.08 (d, 1H, *J* = 8.3 Hz), 10.04 (s, 1H), 9.99 (s, 1H), 9.31 (d, 1H, *J* = 8.7 Hz), 9.25 (d, 1H, *J* = 9.3 Hz), 8.43 (d, 1H, *J* = 8.9 Hz), 8.39 (d, 1H, *J* = 8.2 Hz), 8.30 (t, 1H, *J* = 7.5 Hz), 8.03 (t, 1H, *J* = 7.6 Hz), 7.91 (t, 1H, *J* = 7.9 Hz), 7.71 (t, 1H, *J* = 7.6 Hz), 4.15−4.00 (m, 8H), 3.78 (s, 3H), 3.38 (s, 3H), 1.89−1.84 (m, 9H), 1.81 (t, 3H, *J* = 7.6 Hz). $^1$H NMR (500 MHz, pyrrolidine-$CDCl_3$, aromatic region only): δ 11.15 (s, 1H), 11.07 (s, 1H), 10.29 (d, 1H, *J* = 8.2 Hz), 10.10 (d, 1H, *J* = 8.3 Hz), 9.92 (s, 1H), 9.88 (s, 1H), 9.07 (d, 1H, *J* = 8.3 Hz), 9.00 (d, 1H, *J* = 8.9 Hz), 8.23 (d, 1H, *J* = 8.6 Hz), 8.19 (d, 1H, *J* = 8.2 Hz), 8.12 (t, 1H, *J* = 7.5 Hz), 7.89 (t, 1H, *J* = 7.5 Hz), 7.75 (t, 1H, *J* = 7.4 Hz), 7.59 (t, 1H, *J* = 7.5 Hz). HRMS (ESI) *m/z*: $M^+$ calcd for $C_{46}H_{40}N_4Zn$ 712.2544, found 712.2569.

**12,13-Diethyl-7,8,17,18-tetramethylchryso[5,6-*b*]porphyrin (11b).** Tripyrrane dicarboxylic acid **23b** (75.0 mg, 0.176 mmol) was stirred with TFA (1 mL) under nitrogen for 1 min. The mixture was diluted with dichloromethane (15 mL), and chrysopyrrole dialdehyde **19** (57.0 mg, 0.176 mg) was added. Stirring under nitrogen was continued for 2 h. The solution was neutralized by the dropwise addition of triethylamine, DDQ (40 mg, 0.176 mmol) was added, and the mixture was stirred for a further 1 h. The solution was washed with water and evaporated under reduced pressure. The residue was purified on a grade 3 alumina column eluting with dichloromethane. Recrystallization from chloroform−methanol afforded the chrysoporphyrin (38.4 mg, 0.062 mmol, 35%) as purple crystals, mp >300 °C. UV−vis ($CHCl_3$; 1.36 × $10^{-5}$ M): $\lambda_{max}$/nm (log ε) 424 (5.21), 525 (3.91), 564 (4.57), 583 (4.27), 638 (3.55). UV−vis (2% TFA-$CHCl_3$; 1.36 × $10^{-5}$ M): $\lambda_{max}$/nm (log ε) 420 (5.14), 674 (4.15), 628 (4.45). $^1$H NMR (500 MHz, $CDCl_3$): δ 11.27 (s, 1H), 11.12 (s, 1H), 10.16 (d, 1H, *J* = 8.3 Hz), 10.02 (s, 1H), 10.00 (d, 1H, *J* = 8.8 Hz), 9.97 (s, 1H), 9.11 (d, 1H, *J* = 8.0 Hz), 9.03 (d, 1H, *J* = 8.8 Hz), 8.28 (d, 1H, *J* = 8.9 Hz), 8.24 (d, 1H, *J* = 7.9 Hz), 8.14 (t, 1H, *J* = 7.5 Hz), 7.93 (t, 1H, *J* = 7.5 Hz), 7.80 (t, 1H, *J* = 7.4 Hz), 7.58 (t, 1H, *J* = 7.5 Hz), 4.04−3.99 (m, 4H), 3.81 (s, 3H), 3.70 (s, 3H), 3.62 (s, 3H), 3.37 (s, 3H), 1.93−1.89 (m, 6H), −3.42 (br s, 2H). $^1$H NMR (500 MHz, TFA-$CDCl_3$): δ 11.75 (s, 1H, 5-H), 11.36 (s, 1H, 20-H), 10.56 (s, 1H), 10.53 (s, 1H) (10,15-H), 9.98 (d, 1H, *J* = 8.1 Hz, $2^1$-H), 9.47 (d, 1H, *J* = 8.3 Hz, $3^1$-H), 9.26 (d, 1H, *J* = 8.3 Hz, $2^4$-H), 9.14 (d, 1H, *J* = 8.9 Hz, $3^6$-H), 8.51 (d, 1H, *J* = 8.8 Hz, $3^5$-H), 8.38 (t, 1H, *J* = 7.5 Hz, $2^2$-H), 8.33 (d, 1H, *J* = 8.0 Hz, $3^4$-H), 8.25 (t, 1H, *J* = 7.6 Hz, $2^3$-H), 7.90 (t, 1H, *J* = 7.4 Hz, $3^3$-H), 7.68 (t, 1H, *J* = 7.6 Hz, $3^2$-H), 4.17−4.11 (m, 4H, 2 × $CH_2CH_3$), 3.64 (s, 3H, 18-Me), 3.60 (s, 3H, 17-Me), 3.55 (s, 3H, 8-Me), 3.29 (s, 3H, 7-Me), 1.80−1.74 (2 overlapping triplets, 6H, 2 × $CH_2CH_3$), −2.43 (s, 1H), −2.53 (br s, 1H), −3.63 (v br s, 1H), −3.68 (br s, 1H) (4 × NH). $^{13}C\{^1H\}$ NMR (125 MHz, TFA-$CDCl_3$): δ 144.21, 144.19, 143,9, 143.15, 143,12, 142.2, 142.0, 140.9, 139.1, 138.8, 138.45, 138.42, 137.5, 134.2, 133.5, 132.4, 132.0, 131.0 ($3^5$-CH), 130.2, 129.9 ($2^3$-CH), 129.7 ($2^2$-CH), 129.2, 128.71, 128.69 ($3^3$- and $3^4$-CH)), 127.9 ($3^1$-CH), 127.7, 127.0 ($2^1$-CH), 126.5 ($3^2$-CH), 125.6 ($2^4$-H), 124.9, 121.7 ($3^6$-CH), 100.6 (5-CH), 100.3 (20-CH), 98.7, 98.3 (10,15-CH), 20.1, 17.44, 17.38, 12.23, 12.14, 12.05, 11.69 (7-Me). HRMS (ESI) *m/z*: $[M + H]^+$ calcd for $C_{44}H_{39}N_4$ 623.3169, found 623.3179.

**12,13-Diethyl-8,17-dihexyl-7,18-dimethylchryso[5,6-*b*]-porphyrin (11c).** Hexyl substituted tripyrrane **23c** (222 mg, 0.392 mmol) was dissolved in 2 mL of TFA and stirred under $N_2$ for 2 min. The mixture was diluted with dichloromethane (42 mL), chrysopyrrole dialdehyde **19** (127 mg, 0.393 mmol) was immediately added, and stirring under nitrogen was continued for 2 h. The resulting solution was neutralized by the dropwise addition of triethylamine, DDQ (92 mg, 0.405 mmol) was added, and the mixture was allowed to stir for an additional 1 h. The mixture was washed with 5% sodium bicarbonate and extracted with dichloromethane. After removing the dichloromethane under reduced pressure, the residue was purified on grade 3 alumina eluting with dichloromethane to give a dark purple band. The product was further purified by column chromatography on grade 3 alumina eluting with 70:30 hexanes−dichloromethane and recrystallization from chloroform−methanol to afford the chrysoporphyrin **11c** (132 mg, 0.1730 mmol, 44%) as dark magenta crystals, mp 237.9−238.2 °C. UV−vis ($CH_2Cl_2$; 1.281 × $10^{-5}$ M): $\lambda_{max}$/nm (log ε) 404 (sh, 5.01), 425 (5.21), 523 (3.89), 563 (5.53), 582 (4.25), 637 (3.48). UV−vis (150 equiv TFA-$CH_2Cl_2$; 1.281 × $10^{-5}$ M): $\lambda_{max}$/nm (log ε) 272 (4.59), 348 (4.31), 422 (5.14), 574 (4.14), 598 (4.03), 626 (4.36). UV−vis (5% TFA-$CH_2Cl_2$): 1.281 × $10^{-5}$ M): $\lambda_{max}$/nm (log ε) 410 (5.16), 578 (4.10), 630 (4.32). $^1$H NMR (500 MHz, $CDCl_3$): δ 11.26 (s, 1H), 11.03 (s, 1H), 10.05 (d, 1H, *J* = 8.2 Hz), 10.001 (s, 1H), 9.999 (d, 1H, *J* = 8.8 Hz), 9.97 (s, 1H), 9.02 (d, 1H, *J* = 8.3 Hz), 8.95 (d, 1H, *J* = 8.9 Hz), 8.23−8.20 (m, 2H), 8.06 (t, 1H, *J* = 7.4 Hz), 7.85 (t, 1H, *J* = 7.5 Hz), 7.79 (t, 1H, *J* = 7.4 Hz), 7.58 (t, 1H, *J* = 7.5 Hz), 4.11−3.99 (m, 8H), 3.73 (s, 3H), 3.36 (s, 3H), 2.34−2.25 (m, 4H), 1.95−1.90 (2 overlapping triplets, 6H), 1.56−1.48 (m, 4H), 1.43−1.34 (m, 4H), 0.95−0.91 (2 overlapping triplets, 6H), −3.29 (s, 2H). $^1$H NMR (500 MHz, TFA-$CDCl_3$): δ 11.84 (s, 1H), 11.44 (s, 1H), 10.63 (s, 1H), 10.59 (s, 1H), 9.99 (d, 1H, *J* = 8.1 Hz), 9.52 (d, 1H, *J* = 8.4 Hz), 9.27 (d, 1H, *J* = 8.4 Hz), 9.15 (d, 1H, *J* = 9.0 Hz), 8.52 (d, 1H, *J* = 8.9 Hz), 8.38 (t, 1H, *J* = 7.5 Hz), 8.35 (d, 1H, *J* = 8.0 Hz), 8.25 (t, 1H, *J* = 7.5 Hz), 7.92 (t, 1H, *J* = 7.4 Hz), 7.70 (t, 1H, *J* = 7.5 Hz), 4.20−4.13 (m, 4H), 4.10 (t, 2H, *J* = 7.9 Hz), 4.05 (t, 2H, *J* = 7.9 Hz), 3.68 (s, 3H), 3.34 (s, 3H), 2.18 (pentet, 2H, *J* = 7.7 Hz), 2.09 (pentet, 2H, *J* = 7.7 Hz), 1.86−1.80 (2 overlapping triplets, 6H), 1.74 (pentet, 2H, *J* = 7.5 Hz), 1.66 (pentet, 2H, *J* = 7.5 Hz), 1.56−1.33 (m, 8H), 0.95 (t, 3H, *J* = 7.3 Hz), 0.91 (t, 3H, *J* = 7.3 Hz), −2.73 (br s, 2H), −3.79 (br s, 2H). $^{13}C\{^1H\}$ NMR (125 MHz, $CDCl_3$): δ 152.8, 148.9, 148.6, 144.4, 138.4, 138.2, 138.0, 137.4, 137.2, 137.0, 136.0, 134.2, 133.9, 133.8, 131.8, 130.5, 130.4, 129.69, 129.67, 127.87, 127.86, 127.4, 127.3, 126.7, 126.3, 126.1, 125.0, 124.8, 122.0, 100.7, 100.1, 97.0, 96.8, 33.08, 33.04, 32.16, 32.11, 29.8, 26.57, 26.53, 22.92, 22.90, 20.1, 18.7, 14.35, 14.32, 12.0, 11.5. $^{13}C\{^1H\}$ NMR (125 MHz, TFA-$CDCl_3$): δ 144.67, 144.65, 144.0, 143.8, 143.7, 143.5, 143.0, 142.4, 142.1, 141.3, 139.3, 139.2, 138.7, 138.1, 134.5, 133.8, 132.9, 132,2, 131.3, 130.4, 130.1, 129.9, 128.9, 128.8, 127.9, 127.1, 126.6, 125.8, 125.0, 121.8, 101.1, 100.8, 98.9, 98.5, 32.39, 32.36, 31.9, 31.8, 30.0, 29.9, 27.15, 27.10, 22.77, 22.72, 20.3, 17.22, 17.17, 13.89, 13.84, 12.0, 11.6. HRMS (ESI) *m/z*: $[M + H]^+$ calcd for $C_{54}H_{59}N_4$ 763.4734, found 763.4728.

**[12,13-Diethyl-8,17-dihexyl-7,18-dimethylchryso[5,6-*b*]-porphyrinato]nickel(II) (26d).** Chrysoporphyrin **11c** (10.1 mg, 0.0134 mmol) was dissolved in DMF (10 mL), nickel(II) acetate



https://doi.org/10.1021/acs.joc.2c01859
J. Org. Chem. 2022, 87, 16276−16296

tetrahydrate (7.8 mg) was added, and the mixture was stirred under reflux overnight. The solvent was removed on a rotary evaporator with the aid of an oil pump, and the residue was chromatographically purified on grade 3 alumina eluting with 2:3 dichloromethane−hexanes and recrystallized with chloroform−methanol to afford the nickel complex (8.2 mg, 0.010 mmol, 75%) as a purple solid, mp 180.9−181.6 °C. UV−vis ($CHCl_3$; $1.216 \times 10^{-5}$ M): $\lambda_{max}$/nm (log $\varepsilon$) 417 (5.17), 539 (3.97), 586 (4.65). $^1$H NMR (500 MHz, $CDCl_3$): $\delta$ 10.574 (s, 1H), 10.569 (s, 1H) (5,20-H), 9.72 (d, 1H, $J$ = 8.2 Hz, $2^1$-H), 9.65 (s, 1H), 9.59 (s, 1H) (10,15-H), 9.26 (d, 1H, $J$ = 8.5 Hz, $3^1$-H), 9.10 (d, 1H, $J$ = 8.4 Hz, $2^4$-H), 9.04 (d, 1H, $J$ = 8.9 Hz, $3^6$-H), 8.27 (d, 1H, $J$ = 8.9 Hz, $3^5$-H), 8.16 (d, 1H, $J$ = 8.0 Hz, $3^4$-H), 8.04 (t, 1H, $J$ = 7.5 Hz, $2^2$-H), 7.88 (t, 1H, $J$ = 7.6 Hz, $2^3$-H), 7.66 (t, 1H, $J$ = 7.4 Hz, $3^3$-H), 7.29 (t, 1H, $J$ = 7.6 Hz, $3^2$-H), 3.93−3.87 (m, 6H), 3.77 (t, 2H, $J$ = 7.6 Hz) (8,12,13,17-$CH_2$), 3.54 (s, 3H), 3.06 (s, 3H), 2.23 (pentet, 2H, $J$ = 7.5 Hz), 2.13 (pentet, 2H, $J$ = 7.5 Hz) (8,17-$CH_2CH_2$), 1.86−1.81 (2 overlapping triplets, 6H, 12,13-$CH_2CH_3$), 1.65 (pentet, 2H, J = 7.5 Hz), 1.54 (pentet, 2H, $J$ = 7.5 Hz) (8,17-$CH_2CH_2CH_2$), 1.49−1.40 (m, 6H), 1.36 (sextet, 2H, $J$ = 7.3 Hz) (2 × $CH_2CH_2CH_3$), 0.96 (t, 3H, $J$ = 7.3 Hz), 0.91 (t, 3H, $J$ = 7.3 Hz) ($2(CH_2)_3CH_3$). $^{13}$C{$^1$H} NMR (125 MHz, $CDCl_3$): $\delta$ 143.20, 143.17, 142.6, 142.3, 141.90, 141.87, 141.3, 141.21, 141.18, 141.0, 138.0, 137.39, 137.36, 137.1, 135.8, 135.4, 133.7, 131.5, 130.1, 129.46, 129.38 ($3^1$-CH), 129.0, 128.18 ($2^2$-CH), 128.12 ($3^4$-CH), 127.9 ($3^5$-CH), 127.2 ($3^2$-CH), 126.4, 126.35 ($2^1$ and $2^3$-CH), 125.4, 125.08 ($2^4$-CH), 125.01 ($3^2$-CH), 122.1 ($3^6$-CH), 99.9, 99.4 (5,20-CH), 97.5, 97.3 (10,15-CH), 33.1, 33.0, 32.2, 32.1, 30.0, 29.9, 26.8, 26.7, 22.94, 22.87, 19.95, 19.93, 18.3, 14.29, 14.23, 12.0, 11.4. HRMS (ESI) $m/z$: $M^+$ calcd for $C_{54}H_{56}N_4Ni$ 818.3858, found 818.3828.

**8,17-Diethyl-7,18-dimethylchryso[5,6-*b*]acenaphtho[1,2-*l*]-porphyrin (27).** Acenaphthotripyrrane **28**[18] (80 mg, 0.126 mmol) was stirred with TFA (1 mL) in the dark under nitrogen for 5−6 min. The mixture was diluted with dichloromethane (15 mL), and chrysopyrrole dialdehyde **19** (40.8 mg, 0.126 mg) was added. Stirring under nitrogen was continued for 2 h. The solution was neutralized by the dropwise addition of triethylamine, DDQ (29.2 mg, 0.13 mmol) was added, and the mixture was stirred for a further 1 h. The solution was washed with water and evaporated under reduced pressure. The residue was purified on a grade 3 alumina column, eluting with dichloromethane, and a dark green fraction was collected. Recrystallization from chloroform−methanol afforded acenaphthochrysoporphyrin **27** (26.9 mg, 0.0375 mmol, 30%) as dark purple crystals, mp >300 °C. UV−vis (1% $Et_3N$−$CHCl_3$; $1.396 \times 10^{-5}$ M): $\lambda_{max}$/nm (log $\varepsilon$) 440 (4.87), 591 (sh, 4.30), 621 (4.50), 657 (sh, 3.72), 684 (3.73). UV−vis (2% TFA-$CHCl_3$; $1.396 \times 10^{-5}$ M): $\lambda_{max}$/nm (log $\varepsilon$) 464 (4.84), 588 (4.21), 666 (4.50). $^1$H NMR (500 MHz, TFA-$CDCl_3$): $\delta$ 11.74 (s, 1H, 5-H), 11.33 (s, 1H), 20-H, 10.99 (s, 1H), 10.95 (s, 1H) (10,15-H), 9.95 (d, 1H, 8.2 Hz), 9.53 (d, 1H, $J$ = 8.3 Hz), 9.26 (d, 1H, $J$ = 8.3 Hz), 9.15−9.12 (m, 3H), 8.51 (d, 1H, $J$ = 8.8 Hz), 8.38 (t, 1H, $J$ = 7.5 Hz), 8.34−8.31 (m, 3H), 8.25 (t, 1H, $J$ = 7.6 Hz), 8.14−8.11 (two overlapping doublets, $J$ = 7.5 Hz), 7.92 (t, 1H, $J$ = 7.3 Hz), 7.72 (t, 1H, $J$ = 7.6 Hz), 4.18 (q, 2H, $J$ = 7.8 Hz), 4.14 (q, 2H, $J$ = 7.8 Hz), 3.68 (s, 3H), 3.33 (s, 3H), 1.84 (t, 3H, $J$ = 7.8 Hz), 1.71 (t, 3H, $J$ = 7.8 Hz), −1.92 (br s, 2H), −3.06 (br s, 1H). $^{13}$C{$^1$H} NMR (125 MHz, TFA-$CDCl_3$): $\delta$ 144.7, 144.5, 144.0, 143.4, 142.7, 141.8, 139.7, 138.5, 138.4, 137.8, 136.7, 136.0, 135.8, 134.2, 133.5, 132.5, 131.9, 131.4, 131.2, 131.1, 130.1, 129.9, 129.7, 129.5, 129.3, 128.7, 127.9, 127.7, 127.11, 127.07, 126.9, 126.5, 125.6, 125.0, 121.7, 100.9, 100.48, 100.45, 100.1, 20.4, 20.35, 16.5, 12.0, 11.5. HRMS (ESI) $m/z$: $[M + H]^+$ calcd for $C_{52}H_{39}N_4$ 719.3169, found 719.3170.

**12,13-Diethyl-8,17-dihexyl-7,18-dimethylpyreno[4,5-*b*]-porphyrin (34).** Hexyl substituted tripyrrane **23c** (102.2 mg, 0.181 mmol) was dissolved in TFA (1 mL) under $N_2$ for 2 min. The mixture was diluted with dichloromethane (19 mL), pyrenopyrrole dialdehyde **35**[27] (52.6 mg, 0.177 mmol) was immediately added, and stirring under nitrogen was continued for 2 h. The resulting solution was neutralized by the dropwise addition of triethylamine, DDQ (41.2 mg, 0.181 mmol) was added, and the resulting mixture was stirred for an additional 1 h. The mixture was washed with 5% sodium bicarbonate and extracted with dichloromethane. After removal of the dichloromethane under reduced pressure, the residue was purified on a grade 3 alumina column eluting with dichloromethane to give a dark pink band. The product was further purified by column chromatography on grade 3 alumina eluting with 3:1 hexanes−dichloromethane and recrystallized from chloroform−methanol to afford the pyrenoporphyrin (41.2 mg, 0.056 mmol, 32%) as dark purple crystals, mp 218.5−219.7 °C. UV−vis ($CH_2Cl_2$; $1.286 \times 10^{-5}$ M): $\lambda_{max}$/nm (log $\varepsilon$) 339 (4.48), 383 (4.76), 397 (sh, 4.85), 419 (5.26), 519 (3.89), 558 (4.51), 579 (4.16), 634 (3.29). UV−vis (50 equiv TFA-$CH_2Cl_2$; $1.286 \times 10^{-5}$ M): $\lambda_{max}$/nm (log $\varepsilon$) 270 (4.53), 421 (5.29), 434 (5.19), 569 (4.21), 590 (4.00), 617 (4.26). UV−vis (10% TFA-$CH_2Cl_2$; $1.286 \times 10^{-5}$ M): $\lambda_{max}$/nm (log $\varepsilon$) 313 (4.30), 400 (5.02), 419 (5.19), 435 (sh, 4.97), 573 (4.24), 615 (4.11). $^1$H NMR (500 MHz, $CDCl_3$, 55 °C): $\delta$ 10.59 (s, 2H, 5,20-H), 9.86 (s, 2H, 10,15-H), 9.76 (d, 2H, $J$ = 7.6 Hz, $2^1$,$3^1$-H), 8.20 (d, 2H, $J$ = 7.2 Hz, $2^3$,$3^3$-H), 8.17 (t, 2H, $J$ = 7.4 Hz, $2^2$,$3^2$-H), 8.10 (s, 2H, $2^4$,$3^4$-H), 4.02 (q, 4H, $J$ = 7.8 Hz, 12,13-$CH_2$), 3.94 (t, 4H, $J$ = 7.8 Hz, 8,17-$CH_2$), 3.44 (s, 6H, 7,18-Me), 2.27 (pentet, 4H, $J$ = 7.6 Hz, 8,17-$CH_2CH_2$), 1.97 (t, 6H, $J$ = 7.8 Hz, 12,13-$CH_2CH_3$), 1.75 (pentet, 4H, $J$ = 7.5 Hz, 8,17-$CH_2CH_2CH_2$), 1.54 (pentet, 4H, $J$ = 7.4 Hz, 2 × $CH_2CH_2CH_3$), 1.42 (sextet, 4H, $J$ = 7.4 Hz, 2 × $CH_2CH_2CH_3$), 0.95 (t, 6H, $J$ = 7.3 Hz, 2 × $CH_2CH_2CH_3$), −3.98 (br s, 2H). $^1$H NMR (500 MHz, TFA-$CDCl_3$): $\delta$ 11.76 (s, 2H, 5,20-H), 10.70 (s, 2H, 10,15-H), 10.28 (dd, 2H, $J$ = 1.5, 7.2 Hz, $2^1$,$3^1$-H), 8.74 (dd, 2H, $J$ = 1.6, 7.6 Hz, $2^3$,$3^3$-H), 8.72 (t, 2H, $J$ = 7.6 Hz, $2^2$,$3^2$-H), 8.45 (s, 2H, $2^4$,$3^4$-H), 4.19 (q, 4H, $J$ = 7.7 Hz, 12,13-$CH_2$), 4.15 (t, 4H, $J$ = 7.9 Hz, 8,17-$CH_2$), 3.78 (s, 6H, 7,18-Me), 2.19 (pentet, 4H, $J$ = 7.6 Hz, 8,17-$CH_2CH_2$), 1.80 (t, 6H, $J$ = 7.7 Hz, 12,13-$CH_2CH_3$), 1.74 (pentet, 4H, $J$ = 7.6 Hz, 8,17-$CH_2CH_2CH_2$), 1.55−1.49 (m, 4H, 2 × $CH_2CH_2CH_3$), 1.39 (sextet, 4H, $J$ = 7.5 Hz, 2 × $CH_2CH_2CH_3$), 0.93 (t, 6H, $J$ = 7.4 Hz, 2 × $CH_2CH_2CH_3$), −3.07 (br s, 2H), −3.66 (br s, 1H), −4.04 (br s, 1H). $^{13}$C{$^1$H} NMR (125 MHz, $CDCl_3$): $\delta$ 151.7, 147.7, 144.0, 138.3, 138.2, 137.7, 135.8, 133.9, 132.5, 128.6, 128.0 ($2^4$,$3^4$-CH), 126.5 ($2^2$,$3^2$-CH), 125.8, 125.2 ($2^3$,$3^3$-CH), 123.4 ($2^1$,$3^1$-CH), 99.8 (5,20-CH), 96.8 (10,15-CH), 33.1 (8,17-$CH_2CH_2$), 32.2 (2 × $CH_2CH_2CH_3$), 29.9 (8,17-$CH_2CH_2CH_2$), 26.6 (8,17-$CH_2$), 22.9 (2 × $CH_2CH_2CH_3$), 20.1 (12,13-$CH_2$), 18.7 (12,13-$CH_2CH_3$), 14.3 (2 × $CH_2CH_2CH_3$), 11.7 (7,18-Me). $^{13}$C{$^1$H} NMR (125 MHz, TFA-$CDCl_3$): $\delta$ 144.9, 144.4, 143.4, 143.1, 142.3, 139.1, 139.0, 133.4, 131.5, 129.4 ($2^3$,$3^3$-CH), 129.0 ($2^4$,$3^4$-CH), 128.4 ($2^2$,$3^2$-CH), 127.6, 126.8, 125.3 ($2^1$,$3^1$-CH), 100.8 (5,20-CH), 99.0 (10,15-CH), 32.5 (8,17-$CH_2CH_2$), 31.9 (2 × $CH_2CH_2CH_3$), 30.0 (8,17-$CH_2CH_2CH_2$), 27.2 (8,17-$CH_2$), 22.8 (2 × $CH_2CH_2CH_3$), 20.3 (12,13-$CH_2$), 17.2 (12,13-$CH_2CH_3$), 13.8 (2 × $CH_2CH_2CH_3$), 12.2 (7,18-Me). HRMS (ESI) $m/z$: $[M + H]^+$ calcd for $C_{52}H_{57}N_4$ 737.4578, found 737.4554.

**Benzopyrene-Fused Porphyrin 12c.** Chrysoporphyrin **11c** (50.2 mg, 0.0659 mmol) and approximately 5 equiv of ferric chloride hexahydrate (83.5 mg, 0.31 mmol) were taken up in dichloromethane (24 mL), and the mixture was purged with nitrogen. The stirred mixture was refluxed for 5.5 h, and the progress of the reaction was monitored by TLC. The mixture was washed with water, extracted with dichloromethane, and dried over anhydrous sodium sulfate. The solvent was evaporated under reduced pressure, and the residue was purified by column chromatography on grade 3 alumina eluting with 2:3 dichloromethane−hexanes. Recrystallization from chloroform−methanol afforded the benzopyrene-fused porphyrin (32 mg, 0.042 mmol, 64%) as dark purple crystals, mp >300 °C. UV−vis ($CH_2Cl_2$; $1.265 \times 10^{-5}$ M): $\lambda_{max}$/nm (log $\varepsilon$) 348 (4.38), 441 (sh, 4.69), 467 (5.17), 558 (3.82), 608 (3.83), 683 (3.98). UV−vis (50 equiv TFA-$CH_2Cl_2$; $1.265 \times 10^{-5}$ M): $\lambda_{max}$/nm (log $\varepsilon$) 347 (4.38), 455 (sh, 4.66), 486 (5.18), 616 (sh, 3.76), 700 (4.30). $^1$H NMR (500 MHz, $CDCl_3$): $\delta$ 10.78 (s, 1H, 20-H), 10.14 (d, 1H, $J$ = 8.1 Hz, $2^1$-H), 10.08 (s, 1H), 9.81 (s, 1H) (10,15-H), 9.36 (d, 1H, $J$ = 8.2 Hz, $2^4$-H), 9.08 (d, 1H, $J$ = 9.0 Hz), 9.02 (d, 1H, $J$ = 7.4 Hz, $5^1$-H), 8.41 (d, 1H, $J$ = 8.8 Hz), 8.28 (d, 1H, $J$ = 7.4 Hz, $5^3$-H), 8.26 (t, 1H, $J$ = 7.5 Hz, $2^2$-H), 8.20 (t, 1H, $J$ = 7.5 Hz, $5^2$-H), 8.05 (t, 1H, $J$ = 7.5 Hz, $5^3$-H), 4.05−3.95 (m, 8H, 8,12,13,17-$CH_2$), 3.67 (s, 3H, 18-Me), 3.24 (s, 3H, 7-Me), 2.31 (pentet, 2H, $J$ = 7.5 Hz, 8,17-$CH_2CH_2$), 2.13 (pentet, 2H, $J$ = 7.6 Hz,), 1.95−1.90 (2 overlapping triplets, 6H), 1.76 (pentet, 4H, $J$


https://doi.org/10.1021/acs.joc.2c01859
J. Org. Chem. 2022, 87, 16276−16296

= 7.4 Hz), 1.56−1.48 (m, 4H), 1.40 (sextet, 4H, $J$ = 7.4 Hz), 0.95−0.91 (2 overlapping triplets, 6H), −2.23 (br s, 2H). $^1$H NMR (500 MHz, $CDCl_3$): $\delta$ 10.93 (s, 1H), 10.33 (s, 1H), 10.26 (d, 1H, $J$ = 8.2 Hz), 9.88 (s, 1H), 9.67 (d, 1H, $J$ = 7.5 Hz), 9.61 (d, 1H, $J$ = 8.2 Hz), 9.44 (d, 1H, $J$ = 8.7 Hz), 8.89 (d, 1H, $J$ = 8.9 Hz), 8.76 (d, 1H, $J$ = 7.7 Hz), 8.64 (t, 1H, $J$ = 7.6 Hz), 8.56 (t, 1H, $J$ = 7.3 Hz), 8.34 (t, 1H, $J$ = 7.7 Hz), 4.04−3.85 (m, 6H), 3.73−3.61 (m, 2H), 3.61 (s, 3H), 3.10 (s, 3H), 2.22−2.15 (m, 2H), 1.89−1.18 (m, xH), 0.96−0.89 (2 overlapping triplets, 6H), −0.96 (br s, 2H). $^{13}$C{$^1$H} NMR (125 MHz, $CDCl_3$): $\delta$ 140.5, 139.4, 132.5, 130.7, 130.50, 130.47, 128.3, 128.1, 127.8, 126.7, 126.5, 125.7, 125.6, 125.2, 122.3, 121.7, 121.5, 108.5, 101.4, 99.6, 97.0, 33.0, 32.9, 32.2, 32.1, 30.1, 29.9, 26.9, 26.5, 22.9, 20.08, 20.05, 18.8, 18.7, 16.5, 14.3, 11.9. $^{13}$C{$^1$H} NMR (125 MHz, TFA-$CDCl_3$): $\delta$ 146.9, 146.1, 145.2, 144.3, 143.5, 143.1, 142.0, 141.9, 139.8, 138.59, 138.57, 137.7, 136.6, 134.1, 133.3, 131.9, 131.5, 130.4, 129.8, 129.6, 129.5, 129.0, 128.8, 128.5, 128.2, 126.7, 126.5, 126.2, 123.5, 123.3, 122.3, 120.2, 109.8, 107.2, 98.0, 97.1, 32.2, 32.0, 31.9, 31.7, 30.0, 29.9, 27.0, 26.9, 22.8, 20.2, 19.7, 17.4, 16.9, 14.00, 13.98, 13.4, 12.0. HRMS (ESI) $m/z$: $[M + H]^+$ calcd for $C_{54}H_{57}N_4$ 761.4578, found 761.4549.

**Benzo[*b*]-21-carbaporphyrin (38).** 2,5-Pyrroledicarbaldehyde[40] (22.6 mg, 0.183 mmol) was dissolved with stirring in dichloromethane (20 mL). TFA (1 mL) was added, followed by carbatripyrrin **36**[31] (50 mg, 0.184 mmol), and the mixture was stirred for 30 min. The solution was diluted with dichloromethane, washed with water and 5% sodium bicarbonate solution, and dried over sodium sulfate. The drying agent was removed by suction filtration, and the solvent evaporated under reduced pressure. The residue was run through a silica column, eluting with dichloromethane, and the product recrystallized from chloroform−methanol to give unsubstituted benzocarbaporphyrin **38** (12.0 mg, 0.0334 mmol, 18%) as a red-brown solid, mp >300 °C. UV−vis ($CH_2Cl_2$; 1.667 × $10^{-5}$ M): $\lambda_{max}$/nm (log $\varepsilon$) 382 (sh, 4.49), 418 (5.05), 503 (4.18), 534 (sh, 3.62), 602 (3.52), 660 (2.89). UV−vis (100 eq TFA-$CH_2Cl_2$; 1.667 × $10^{-5}$ M): $\lambda_{max}$/nm (log $\varepsilon$) 297 (4.30), 397 (4.69), 421 (4.76), 470 (4.20), 543 (3.90), 606 (3.72), 665 (3.43). UV−vis (1% TFA-$CH_2Cl_2$; 1.667 × $10^{-5}$ M): $\lambda_{max}$/nm (log $\varepsilon$) 298 (4.33), 398 (4.71), 430 (4.72), 472 (sh, 4.23), 545 (3.89), 610 (3.75), 674 (3.40). $^1$H NMR (500 MHz, $CDCl_3$): $\delta$ 10.29 (s, 2H, 5,20-H), 10.03 (s, 2H, 10,15-H), 9.43 (d, 2H, $J$ = 4.6 Hz, 7,18-H), 9.34 (d, 2H, $J$ = 4.6 Hz, 8,17-H), 9.29 (s, 2H, 12,13-H), 8.86−8.83 (m, 2H, $2^1$,$3^1$-H), 7.80−7.77 (m, 2H, $2^2$,$3^2$-H), −3.87 (br s, 2H, 2 × NH), −6.96 (s, 1H, 21-H). $^1$H NMR (500 MHz, 4 $\mu$L TFA-$CDCl_3$, 50 °C): $\delta$ 10.39 (s, 2H, 5,20-H), 10.26 (s, 2H, 10,15-H), 9.41 (s, 2H, 12,13-H), 9.32 (d, 2H, $J$ = 4.5 Hz, 7,18-H), 9.28 (d, 2H, $J$ = 4.5 Hz, 8,17-H), 8.65−8.61 (m, 2H, $2^1$,$3^1$-H), 7.74−7.70 (m, 2H, $2^2$,$3^2$-H), −2.71 (br s, 2H), −7.29 (s, 1H, 21-H). $^{13}$C{$^1$H} NMR (125 MHz, 4 $\mu$L TFA-$CDCl_3$, 50 °C): $\delta$ 143.1, 142.2, 139.6, 139.5, 139.4, 129.2 (12,13-CH), 128.8 ($2^2$,$3^2$-CH), 127.8 (2 × pyrrole-CH), 127.6 (2 × pyrrole-CH), 121.8 ($2^1$,$3^1$-CH), 121.6 (21-CH), 108.8 (5,20-CH), 102.0 (10,15-CH). HRMS (ESI) $m/z$: $[M + H]^+$ calcd for $C_{25}H_{18}N_3$ 360.1495, found 360.1496.

**Benzo[*b*]chryso[5,6-*l*]-21-carbaporphyrin (40).** Chrysopyrrole dialdehyde **19** (59.4 mg, 0.184 mmol) was dissolved with stirring in dichloromethane (20 mL). TFA (1 mL) was added, followed by carbatripyrrin **36**[31] (50 mg, 0.184 mmol), and the mixture was stirred for 30 min. The solution was diluted with dichloromethane, washed with water and 5% sodium bicarbonate solution, and dried over sodium sulfate. The drying agent was removed by suction filtration, and the solvent evaporated under reduced pressure. The residue was run through a silica column, eluting with dichloromethane, and the product recrystallized from chloroform−methanol to give the chrysobenzocarbaporphyrin (12.6 mg, 0.0225 mmol, 12%) as a dark solid, mp >300 °C. UV−vis (1% $Et_3N$−$CH_2Cl_2$; 1.229 × $10^{-5}$ M): $\lambda_{max}$/nm (log $\varepsilon$) 386 (4.50), 446 (4.99), 518 (4.10), 557 (4.29), 622 (3.70), 744 (3.05). UV−vis (200 equiv TFA-$CH_2Cl_2$; 1.229 × $10^{-5}$ M): $\lambda_{max}$/nm (log $\varepsilon$) 270 (4.69), 409 (4.52), 467 (4.93), 562 (4.05), 601 (3.91), 626 (3.94). $^1$H NMR (500 MHz, 2 $\mu$L TFA-$CDCl_3$, 50 °C): $\delta$ 10.86 (s, 1H), 10.80 (s, 1H), 10.10 (s, 1H), 10.04 (s, 1H), 9.99 (d, 1H, $J$ = 8.0 Hz), 9.82 (d, 1H, $J$ = 8.2 Hz), 9.10−9.03 (m, 3H), 8.94 (d, 1H, $J$ = 8.6 Hz), 8.89−8.87 (m, 1H), 8.58−8.56 (m, 1H), 8.48−8.45 (m, 2H), 8.37 (d, 1H, $J$ = 8.6 Hz), 8.27 (d, 1H, $J$ = 8.2 Hz), 8.21 (t, 1H, $J$ = 7.2 Hz), 8.06 (t, 1H, $J$ = 7.5 Hz), 7.87 (t, 1H, $J$ = 7.4 Hz), 7.75 (t, 1H, $J$ = 7.5 Hz), 7.66−7.63 (m, 2H), −1.31 (br s, 2H), −6.94 (s, 1H). $^{13}$C{$^1$H} NMR (125 MHz, 2 $\mu$L TFA-$CDCl_3$, 50 °C): $\delta$ 143.5, 143.0, 141.9, 141.8, 140.7, 140.4, 138.5, 138.4, 135.5, 133.8, 132.7, 131.4, 130.3, 130.1, 130.0, 129.0, 128.8, 128.61, 128.58, 128.37, 128.33, 128.30, 128.0, 127.2, 127.0, 126.73, 126.67, 126.3, 125.2, 122.9, 121.8, 121.7, 121.4, 109.6, 109.5, 100.47, 100.37. HRMS (ESI) $m/z$: $[M + H]^+$ calcd for $C_{41}H_{26}N_3$ 560.2121, found 560.2137.

**Benzo[*b*]pyreno[4,5-*l*]-21-carbaporphyrin (41).** Pyrenopyrrole dialdehyde **35**[27] (54.6 mg, 0.184 mmol) was dissolved with stirring in dichloromethane (20 mL). TFA (1 mL) was added, followed by carbatripyrrin **36**[31] (50 mg, 0.184 mmol), and the mixture was stirred for 30 min at room temperature. The solution was diluted with dichloromethane, washed with water and 5% sodium bicarbonate solution, and dried over sodium sulfate. The drying agent was removed by suction filtration, and the solvent evaporated under reduced pressure. The residue was run through a silica column, eluting with dichloromethane, and the product recrystallized from chloroform−methanol to give pyreno-benzocarbaporphyrin **41** (14.5 mg, 0.0272 mmol, 15%) as a dark solid, mp >300 °C. UV−vis (1% $Et_3N$−$CH_2Cl_2$; 1.115 × $10^{-5}$ M): $\lambda_{max}$/nm (log $\varepsilon$) 386 (4.64), 441 (5.17), 515 (4.27), 554 (4.37), 617 (3.85), 679 (3.46). UV−vis (100 equiv TFA-$CH_2Cl_2$; 1.115 × $10^{-5}$ M): $\lambda_{max}$/nm (log $\varepsilon$) 383 (sh, 4.44), 407 (4.56), 460 (5.11), 560 (4.16), 625 (4.03). $^1$H NMR (500 MHz, 2 $\mu$L TFA-$CDCl_3$, 55 °C): $\delta$ 11.12 (s, 2H, 10,15-H), 10.85 (s, 2H, 5,20-H), 10.24−10.22 (m, 2H, $12^1$,$13^1$-H), 9.29−9.25 (m, 4H, 7,18-H and $12^3$,$13^3$-H), 8.61−8.58 (m, 2H, $2^1$,$3^1$-H), 8.54−8.51 (m, 4H, 8,17-H and $12^2$,$13^2$-H), 8.27 (s, 2H, $12^4$,$13^4$-H), 7.72−7.69 (m, 2H ($2^2$,$3^2$-H), −1.1 (br s, 2H), −6.44 (s, 1H, 21-CH). HRMS (ESI) $m/z$: $[M + H]^+$ calcd for $C_{39}H_{24}N_3$ 534.1965, found 534.1979.

**Benzo[*b*]acenaphtho[1,2-*l*]-21-carbaporphyrin (42).** Acenaphthopyrrole dialdehyde **39**[18] (45.3 mg, 0.183 mmol) was dissolved with stirring in dichloromethane (20 mL). TFA (1 mL) was added, followed by carbatripyrrin **36**[31] (50 mg, 0.184 mmol), and the mixture was stirred for 30 min at room temperature. The solution was diluted with dichloromethane, washed with water and 5% sodium bicarbonate solution, and dried over sodium sulfate. The drying agent was removed by suction filtration, and the solvent evaporated on a rotary evaporator. The residue was run through a silica column, eluting with dichloromethane, and the product recrystallized from chloroform−methanol to give acenaphtho-carbaporphyrin **42** (13.5 mg, 0.028 mmol, 15%) as a dark solid, mp >300 °C. UV−vis (1% $Et_3N$−$CH_2Cl_2$; 1.600 × $10^{-5}$ M): $\lambda_{max}$/nm (log $\varepsilon$) 391 (4.61), 450 (5.09), 526 (4.15), 567 (4.46), 623 (3.82). UV−vis (50 equiv TFA-$CH_2Cl_2$; 1.600 × $10^{-5}$ M): $\lambda_{max}$/nm (log $\varepsilon$) 298 (4.40), 411 (4.61), 470 (5.18), 494 (sh, 4.51), 567 (4.08), 614 (4.17), 697 (3.49). $^1$H NMR (500 MHz, 4 $\mu$L TFA-$CDCl_3$, 50 °C): $\delta$ 10.47 (s, 2H, 10,15-H), 10.31 (s, 2H, 5,20-H), 9.31−9.29 (AB quartet, 4H, $J$ = 4.7 Hz, 4 × pyrrole-H), 8.95 (d, 2H, $J$ = 6.8 Hz, $12^1$,$13^1$-H), 8.61−8.58 (m, 2H, $2^1$,$3^1$-H), 8.14 (d, 2H, $J$ = 8.0 Hz, $12^3$,$13^3$-H), 7.98 (t, 2H, $J$ = 7.5 Hz, $12^2$,$13^2$-H), 7.72−7.69 (m, 2H, $2^2$,$3^2$-H), −2.38 (br s, 3H), −6.78 (s, 1H, 21-H). This carbaporphyrin was too insoluble to allow a carbon-13 NMR spectrum to be run but partial data could be obtained from the HSQC spectrum: $\delta$ 129.6 ($12^3$,$13^3$-CH), 128.9 ($12^2$,$13^2$-CH), 128.6 ($2^2$,$3^2$-CH), 127.7 (7,8,17,18-CH), 125.0 ($12^1$,$13^1$-CH), 121.6 (21-CH and $2^1$,$3^1$-CH), 108.8 (5,20-CH), 100.5 (10,15-CH). HRMS (ESI) $m/z$: $[M + H]^+$ calcd for $C_{35}H_{22}N_3$ 484.1808, found 484.1826.

**Computational Studies.** Calculations on structures **CP** and **BPP** (6 tautomers each), and related protonated species, were performed using Gaussian 16, Revision C.01.[41] Geometry optimization of these structures was performed with the M06-2X functional and the 6-311++G(d,p) basis set.[42] Vibrational frequencies were computed to confirm the absence of imaginary frequencies to confirm that the structures are minima and to derive zero-point energy and vibrational entropy corrections from unscaled frequencies. Single Point Energy (SPE) calculations were performed on the optimized geometries using the M06-2X functional with a cc-PVTZ basis set.[43] Two types of NMR calculations were performed; the GIAO method was used to obtain NICS values,[44] and CGST was used to obtain ACID plots,[26,45]


https://doi.org/10.1021/acs.joc.2c01859
J. Org. Chem. 2022, 87, 16276−16296

NICS(0) was calculated at the mean position of all the four heavy atoms in the middle of the macrocycle. NICS($a$), NICS($b$), NICS($c$), NICS($d$), NICS($e$), NICS($f$), NICS($g$), NICS($h$), and NICS($i$) values were obtained by applying the same method to the mean position of the heavy atoms that comprise the individual rings of each macrocycle. In addition, NICS$(1)_{zz}$, NICS$(1a)_{zz}$, NICS$(1b)_{zz}$, NICS$(1c)_{zz}$, NICS$(1d)_{zz}$, NICS$(1e)_{zz}$, NICS$(1f)_{zz}$, NICS$(1g)_{zz}$, NICS$(1h)_{zz}$, and NICS$(1i)_{zz}$ were obtained by applying the same method to ghost atoms placed 1 Å above each of the corresponding NICS(0) points and extracting the zz contribution of the magnetic tensor. The resulting Cartesian coordinates, energies, 3D geometries, and AICD plots for all the molecules can be found in the Supporting Information.

## ■ ASSOCIATED CONTENT

### Data Availability Statement

The data underlying this study are available in the published article and its online Supporting Information.

### Supporting Information

The Supporting Information is available free of charge at https://pubs.acs.org/doi/10.1021/acs.joc.2c01859.

Tables giving Cartesian coordinates, calculated energies, selected bond lengths and AICD plots, and selected UV−vis, $^1$H NMR, $^1$H−$^1$H COSY, HSQC, DEPT-135, $^{13}$C{$^1$H} NMR, and mass spectra are provided (PDF)

## ■ AUTHOR INFORMATION


### Corresponding Author

**Timothy D. Lash** − *Department of Chemistry, Illinois State University, Normal, Illinois 61790-4160, United States;* orcid.org/0000-0002-0050-0385; Email: tdlash@ilstu.edu

### Authors

**Melissa A. Mathius** − *Department of Chemistry, Illinois State University, Normal, Illinois 61790-4160, United States*

**Deyaa I. AbuSalim** − *Department of Chemistry, Illinois State University, Normal, Illinois 61790-4160, United States*

Complete contact information is available at: https://pubs.acs.org/10.1021/acs.joc.2c01859


### Notes

The authors declare no competing financial interest.

## ■ ACKNOWLEDGMENTS

This work was supported by the National Science Foundation under Grant CHE-1855240. NSF is also acknowledged for providing funding for the departmental NMR spectrometers (CHE-0722385) and mass spectrometer (CHE-1337497) under the Major Research Instrumentation (MRI) program.

## ■ REFERENCES


(1) Matsuoka, W.; Ito, H.; Sarlah, D.; Itami, K. Diversity-orientated Synthesis of Nanographenes Enabled by Dearomative Annulative π-Extension. *Nature Comm.* **2021**, *12*, 3940. Pozo, I.; Guitián, E.; Pérez, A.; Peña, D. Synthesis of Nanographenes, Starphenes, and Sterically Congested Polyarenes by Aryne Cyclotetramerization. *Acc. Chem. Res.* **2019**, *52*, 2472−2481.

(2) (a) Allard, S.; Forster, M.; Souharce, B.; Thiem, H.; Scherf, U. Organic Semiconductors for Solution-Processable Field-Effect Transistors (OFETs). *Angew. Chem., Int. Ed.* **2008**, *47*, 4070−4098. (b) Wang, C.; Dong, H.; Hu, W.; Liu, Y.; Zhu, D. Semiconducting π-Conjugated Systems in Field-Effect Transistors: a Material Odyssey of Organic Electronics. *Chem. Rev.* **2012**, *112*, 2208−2267.

(3) Panwar, N.; Soehartono, A. M.; Chan, K. K.; Zeng, S.; Xu, G.; Qu, J.; Coquet, P.; Yong, K.-T.; Chen, X. Nanocarbons for Biology and Medicine: Sensing, Imaging, and Drug Delivery. *Chem. Rev.* **2019**, *119*, 9559−9656.

(4) (a) Yang, G.; Liu, L.; Yang, Q.; Wang, S. Tetraacenaphthoporphyrin: A π-Conjugated Porphyrin with Efficient Light-Activated Anticancer Activity. *Chem.—Asian J.* **2011**, *6*, 1147−1150. (b) Gardner, D. M.; Taylor, V. M.; Cedeño, D. L.; Padhee, S.; Robledo, S. M.; Jones, M. A.; Lash, T. D.; Vélez, I. D. Association of Acenaphthoporphyrins with Liposomes for the Photodynamic Treatment of Leishmaniasis. *Photochem. Photobiol.* **2010**, *86*, 645−652.

(5) (a) Stępień, M.; Gonka, E.; Sprutta, N. Heterocyclic Nanographenes and Other Polycyclic Heteroaromatic Compounds: Synthetic Routes, Properties and Applications. *Chem. Rev.* **2017**, *117*, 3479−3716. (b) Borissov, A.; Maurya, M. K.; Moshniaha, L.; Wong, W.-S.; Zyla-Karwowska, M.; Stępień, M. Recent Advances in Heterocyclic Nanographenes and Other Polycyclic Heteroaromatic Compounds. *Chem. Rev.* **2022**, *122*, 565−788. (c) Wang, X.-Y.; Yao, X.; Narita, A.; Müllen, K. Heteroatom-Doped Nanographenes with Structural Precision. *Acc. Chem. Res.* **2019**, *52*, 2491−2505.

(6) (a) Lash, T. D. Syntheses of Novel Porphyrinoid Chromophores. In *The Porphyrin Handbook*; Kadish, K. M., Smith, K. M., Guilard, R., Eds.; Academic Press: San Diego, CA, 2000; Vol. *2*, pp 125−199. (b) Ono, N.; Yamada, H.; Okujima, T. Synthesis of Porphyrins with Fused Aromatic Rings. In *Handbook of Porphyrin Science - With Applications to Chemistry, Physics, Material Science, Engineering, Biology and Medicine*; Kadish, K. M., Smith, K. M., Guilard, R., Eds.;World Scientific Publ.: Singapore, 2010; Vol. *2*, pp 1−102. (c) Cheprakov, A. V. The Synthesis of π-Extended Porphyrins. In *Handbook of Porphyrin Science - With Applications to Chemistry, Physics, Material Science, Engineering, Biology and Medicine*; Kadish, K. M., Smith, K. M., Guilard, R., Eds.; World Scientific Publ.: Singapore, 2011; Vol. *13*, pp 1−149.

(7) (a) Rein, M.; Hanack, M. Synthesis of Iron and Cobalt Complexes of Tetra(2,3-naphtho)porphine. *Chem. Ber.* **1988**, *121*, 1601−1608. (b) Ito, S.; Ochi, N.; Murashima, T.; Ono, N.; Uno, H. A New Synthesis of [2,3]Naphthoporphyrins. *Chem. Commun.* **2000**, *36*, 893−894. (c) Ishii, Y.; Ito, S.; Saito, Y.; Uno, D.; Oba, T. Synthesis of [2,3]Naphthoporphyrins using 4,9-Dihydro-4,9-ethano-2H-benz[*f*]-isoindole as a Benz[*f*]isoindole Equivalent. *Tetrahedron* **2015**, *71*, 8892−8898. (d) Roitman, L.; Ehrenberg, B.; Kobayashi, N. Spectral Properties and Absolute Determination of Singlet Oxygen Production Yield by Naphthaloporphyrins. *J. Photochem. Photobiol., A* **1994**, *77*, 23−28. (e) Finikova, O. S.; Cheprakov, A. V.; Carroll, P. J.; Vinogradov, S. A. Novel Route to Functionalized Tetraaryltetra[2,3]-naphthaloporphyrins via Oxidative Aromatization. *J. Org. Chem.* **2003**, *68*, 7517−7520. (f) Finikova, O. S.; Aleshchenkov, S. E.; Brinas, R. P.; Cheprakov, A. V.; Carroll, P. J.; Vinogradov, S. A. Synthesis of Symmetrical Tetraaryltetranaphtho[2,3]porphyrins. *J. Org. Chem.* **2005**, *70*, 4617−4628. (g) Rozhkov, V. V.; Khajehpour, M.; Vinogradov, S. A. Luminescent Zn and Pd Tetranaphthaloporphyrins. *Inorg. Chem.* **2003**, *42*, 4253−4255.

(8) (a) Kobayashi, N.; Nevin, W. A.; Mizunuma, S.; Awaji, H.; Yamaguchi, M. Ring-expanded Porphyrins as an Approach Towards Highly Conductive Molecular Semiconductors. *Chem. Phys. Lett.* **1993**, *205*, 51−54. (b) Yamada, H.; Kuzuhara, D.; Takahashi, T.; Shimizu, Y.; Uota, K.; Okujima, T.; Uno, H.; Ono, N. Synthesis and Characterization of Tetraanthroporphyrins. *Org. Lett.* **2008**, *10*, 2947−2950. (c) Filatov, M. A.; Baluschev, S.; Ilieva, I. Z.; Enkelmann, V.; Miteva, T.; Landfester, K.; Aleshchenkov, S. E.; Cheprakov, A. V. Tetraaryltetraanthra[2,3]porphyrins: Synthesis, Structure, and Optical Properties. *J. Org. Chem.* **2012**, *77*, 11119−11131.

(9) (a) Lash, T. D.; Novak, B. H. Tetraphenanthro[9,10-*b*:9,10-*g*:9,10-*l*:9,10-*q*]porphyrin, a New Highly Conjugated Porphyrin System. *Angew. Chem., Int. Ed. Engl.* **1995**, *34*, 683−685. (b) Xu, H.-J.; Mack, J.; Descalzo, A. B.; Shen, Z.; Kobayashi, N.; You, X.-Z.;

Rurack, K. *meso*-Aryl Phenanthroporphyrins: Synthesis and Spectroscopic Properties. *Chem.—Eur. J.* **2011**, *17*, 8965−8983.
(10) (a) Lash, T. D.; Chandrasekar, P. Synthesis of Tetraphenyltetraacenaphthoporphyrin, a New Highly Conjugated Porphyrin System with Remarkably Red Shifted Electronic Absorption Spectra. *J. Am. Chem. Soc.* **1996**, *118*, 8767−8768. (b) Mack, J.; Asano, Y.; Kobayashi, N.; Stillman, M. J. Application of MCD Spectroscopy and TD-DFT to a Highly Non-Planar Porphyrinoid Ring System. New Insights on Red-Shifted Porphyrinoid Spectral Bands. *J. Am. Chem. Soc.* **2005**, *127*, 17697−17711.
(11) (a) Barton, D. H. R.; Zard, S. Z. A New Synthesis of Pyrroles from Nitroalkenes. *J. Chem. Soc., Chem. Commun.* **1985**, *21*, 1098−1100. (b) Barton, D. H. R.; Kervagoret, J.; Zard, S. Z. A Useful Synthesis of Pyrroles from Nitroolefins. *Tetrahedron* **1990**, *46*, 7587−7598. (c) Gribble, G. W. Barton−Zard Reaction. In *Name Reactions in Heterocyclic Chemistry*; Li, J. J., Ed.; Wiley: Hoboken, NJ, 2005; pp 70−78.
(12) Lash, T. D.; Novak, B. H.; Lin, Y. Synthesis of Phenanthropyrroles and Phenanthrolinopyrroles from Isocyanoacetates: An Extension of the Barton-Zard Pyrrole Condensation. *Tetrahedron Lett.* **1994**, *35*, 2493−2494.
(13) Ono, N.; Hironaga, H.; Simizu, K.; Ono, K.; Kuwano, K.; Ogawa, T. Synthesis of Pyrroles Annulated with Polycyclic Aromatic Compounds; Precursor Molecules for Low Band Gap Polymers. *J. Chem. Soc., Chem. Commun.* **1994**, *30*, 1019−1020.
(14) Lash, T. D. What's in a Name? The MacDonald Condensation. *J. Porphyrins Phthalocyanines* **2016**, *20*, 855−888 and references cited therein.
(15) Lash, T. D.; Denny, C. P. Porphyrins with Exocyclic rings. Part 5. Synthesis of a Naphtho[1,2-*b*]porphyrin. *Tetrahedron* **1995**, *51*, 59−66.
(16) Ono, N.; Hironaga, H.; Ono, K.; Kaneko, S.; Murashima, T.; Ueda, T.; Tsukamura, C.; Ogawa, T. A New Synthesis of Pyrroles and Porphyrins Fused with Aromatic Rings. *J. Chem. Soc., Perkin Trans. 1* **1996**, 417−423.
(17) (a) Novak, B. H.; Lash, T. D. Porphyrins with Exocyclic Rings. Part 11. Synthesis and Characterization of Phenanthroporphyrins, a New Class of Modified Porphyrin Chromophores. *J. Org. Chem.* **1998**, *63*, 3998−4010. (b) Lash, T. D.; Rauen, P. J. Extended Porphyrinoid Chromophores: Heteroporphyrins Fused to Phenanthrene and Acenaphthylene. *Tetrahedron* **2021**, *100*, 132481 and references cited therein.
(18) Lash, T. D.; Chandrasekar, P.; Osuma, A. T.; Chaney, S. T.; Spence, J. D. Porphyrins with Exocyclic Rings. Part 13. Synthesis and Characterization of Highly Modified Porphyrin Chromophores with Fused Acenaphthylene and Benzothiadiazole Rings. *J. Org. Chem.* **1998**, *63*, 8455−8469.
(19) Lash, T. D. Modification of the Porphyrin Chromophore by Ring Fusion: Identifying Trends due to Annelation of the Porphyrin Nucleus. *J. Porphyrins Phthalocyanines* **2001**, *5*, 267−288 and references cited therein.
(20) Lash, T. D.; Wijesinghe, C.; Osuma, A. T.; Patel, J. R. Synthesis of Novel Porphyrin Chromophores from Nitroarenes: Further Applications of the Barton-Zard Pyrrole Condensation. *Tetrahedron Lett.* **1997**, *38*, 2031−2034.
(21) Tardieux, C.; Bolze, F.; Gros, C. P.; Guilard, R. New One-Step Synthesis of 3,4-Disubstituted Pyrrole-2,5-dicarbaldehydes. *Synthesis* **1998**, *1998*, 267−268.
(22) Dolphin, D.; Paine, J. B., III; Woodward, R. B. Pyrrole Chemistry. The Cyanovinyl Aldehyde Protecting Groups. *J. Org. Chem.* **1976**, *41*, 2830−2835.
(23) Sessler, J. L.; Johnson, M. R.; Lynch, V. Synthesis and Crystal Structure of a Novel Tripyrrane-Containing Porphyrinogens-like Macrocycle. *J. Org. Chem.* **1987**, *52*, 4394−4397.
(24) Lash, T. D. Porphyrins with Exocyclic Rings. Part 9. Porphyrin Synthesis by the "3 + 1" Approach. *J. Porphyrins Phthalocyanines* **1997**, *1*, 29−44.
(25) Schleyer, P. v. R.; Maerker, C.; Dransfeld, A.; Jiao, H.; van Eikema Hommes, N. J. R. Nucleus-Independent Chemical Shifts: a Simple and Efficient Aromaticity Probe. *J. Am. Chem. Soc.* **1996**, *118*, 6317−6318.
(26) Geuenich, D.; Hess, K.; Köhler, F.; Herges, R. Anisotropy of Induced Current Density (ACID), a General Method to Quantify and Visualize Electronic Delocalization. *Chem. Rev.* **2005**, *105*, 3758−3772.
(27) Gandhi, V.; Thompson, M. L.; Lash, T. D. Porphyrins with Exocyclic Rings. Part 24. Synthesis and Spectroscopic Properties of Pyrenoporphyrins, Potential Building Blocks for Porphyrin Molecular Wires. *Tetrahedron* **2010**, *66*, 1787−1799.
(28) (a) Myśliwiec, D.; Donnio, B.; Chmielewski, P. J.; Heinrich, B.; Stępień, M. Peripherally Fused Porphyrins via the Scholl Reaction: Synthesis, Self-Assembly, and Mesomorphism. *J. Am. Chem. Soc.* **2012**, *134*, 4822−4833. (b) Martin, M. M.; Oleszak, C.; Hampel, F.; Jux, N. Oxidative Cyclodehydrogenation Reactions with Tetraarylporphyrins. *Eur. J. Org. Chem.* **2020**, *2020*, 6758−6762. (c) Yamane, O.; Sugiura, K.-i.; Miyasaka, H.; Nakamura, K.; Fujimoto, T.; Nakamura, K.; Kaneda, T.; Sakata, Y.; Yamashita, M. Pyrene-Fused Porphyrins: Annulation Reactions of *meso*-Pyrenylporphyrins. *Chem. Lett.* **2004**, *33*, 40−41. (d) Davis, N. K. S.; Pawlicki, M.; Anderson, H. L. Expanding the Porphyrin $\pi$-System by Fusion with Anthracene. *Org. Lett.* **2008**, *10*, 3945−3947. (e) Davis, N. K. S.; Thompson, A. L.; Anderson, H. L. Bis-Anthracene Fused Porphyrins: Synthesis, Crystal Structure, and Near-IR Absorption. *Org. Lett.* **2010**, *12*, 2124−2127. (f) Kurotobi, K.; Kim, K. S.; Noh, S. B.; Kim, D.; Osuka, A. A Quadruply Azulene-Fused Porphyrin with Intense Near-IR Absorption and a Large Two-Photon Absorption Cross Section. *Angew. Chem., Int. Ed.* **2006**, *45*, 3944−3947.
(29) Nisa, K.; Khatri, V.; Kumar, S.; Arora, S.; Ahmad, S.; Dandia, A.; Thirumal, M.; Kashyap, H. K.; Chauhan, S. M. S. Synthesis and Redox Properties of Superbenzene Porphyrin Conjugates. *Inorg. Chem.* **2020**, *59*, 16168−16177.
(30) Lash, T. D. Carbaporphyrinoid Systems. *Chem. Rev.* **2017**, *117*, 2313−2446.
(31) Stateman, L. M.; Lash, T. D. Syntheses of Carbaporphyrinoid Systems using a Carbatripyrrin Methodology. *Org. Lett.* **2015**, *17*, 4522−4525.
(32) Smolczyk, T. J.; Lash, T. D. Alphabet Soup within a Porphyrinoid Cavity: Synthesis of Heterocarbaporphyrins with CNNO, CNOO, CNSO and CNSeO Cores from an Oxacarbatripyrrin. *Chem. Commun.* **2018**, *54*, 9003−9006.
(33) Man, E. H.; Frostick, F. C., Jr.; Hauser, C. R. Proportions of Isomeric Ketone Enol Acetates from O-Acetylations of Methylmethylene Ketones with Isopropenyl Acetate. *J. Am. Chem. Soc.* **1952**, *74*, 3228−3230.
(34) MacDonald, S. F.; Markovac, A. Higher Homologues of Pyrroles and Dipyrrylmethanes. *Can. J. Chem.* **1965**, *43*, 3247−3252.
(35) Brown, D.; Griffiths, D.; Rider, M. E.; Smith, R. C. Synthesis of *N*-Substituted Prodigiosenes. *J. Chem. Soc., Perkin Trans. 1* **1986**, 455−463.
(36) Sessler, J. L.; Mozaffari, A.; Johnson, M. R. 3,4-Diethylpyrrole and 2,3,7,8,12,13,17,18-Octaethylporphyrin. *Org. Synth.* **1992**, *70*, 68−78.
(37) (a) Clezy, P. S.; Thuc, L. v. The Chemistry of Pyrrolic Compounds. LVII. The Oxidative Cyclization of Derivatives of 1,19-Dideoxybilines-*b*. *Aust. J. Chem.* **1984**, *37*, 2085−2092. (b) Bauer, V. J.; Clive, D. L. J.; Dolphin, D.; Paine, J. B., III; Harris, F. L.; King, M. M.; Loder, J.; Wang, S. W. C.; Woodward, R. B. Sapphyrins: Novel Aromatic Pentapyrrolic Macrocycles. *J. Am. Chem. Soc.* **1983**, *105*, 6429−36.
(38) Clezy, P. S.; Crowley, R. J.; Hai, T. T. The Chemistry of Pyrrolic Compounds. L. The Synthesis of Oxorhodoporphyrin Dimethyl Ester and Some of Its Derivatives. *Aust. J. Chem.* **1982**, *35*, 411−421.
(39) (a) Badger, G. M.; Harris, R. L. N.; Jones, R. A.; Sasse, J. M. Porphyrins. I. Intramolecular Hydrogen Bonding in Pyrromethenes and Porphyrins. *J. Chem. Soc.* **1962**, 4329−4337. (b) Bullock, E.; Johnson, A. W.; Markham, E.; Shaw, K. B. A Synthesis of Coproporphyrin III. *J. Chem. Soc.* **1958**, 1430−1440.


https://doi.org/10.1021/acs.joc.2c01859
*J. Org. Chem.* 2022, 87, 16276−16296

(40) Loader, C. E.; Anderson, H. J. Pyrrole Chemistry. Part XX: Synthesis of Pyrrole Acetals. *Synthesis* **1978**, *1978*, 295−296.
(41) Frisch, M. J.; Trucks, G. W.; Schlegel, H. B.; Scuseria, G. E.; Robb, M. A.; Cheeseman, J. R.; Scalmani, G.; Barone, V.; Petersson, G. A.; Nakatsuji, H.; Li, X.; Caricato, M.; Marenich, A. V.; Bloino, J.; Janesko, B. G.; Gomperts, R.; Mennucci, B.; Hratchian, H. P.; Ortiz, J. V.; Izmaylov, A. F.; Sonnenberg, J. L.; Williams-Young, D.; Ding, F.; Lipparini, F.; Egidi, F.; Goings, J.; Peng, B.; Petrone, A.; Henderson, T.; Ranasinghe, D.; Zakrzewski, V. G.; Gao, J.; Rega, N.; Zheng, G.; Liang, W.; Hada, M.; Ehara, M.; Toyota, K.; Fukuda, R.; Hasegawa, J.; Ishida, M.; Nakajima, T.; Honda, Y.; Kitao, O.; Nakai, H.; Vreven, T.; Throssell, K.; Montgomery, J. A., Jr.; Peralta, J. E.; Ogliaro, F.; Bearpark, M. J.; Heyd, J. J.; Brothers, E. N.; Kudin, K. N.; Staroverov, V. N.; Keith, T. A.; Kobayashi, R.; Normand, J.; Raghavachari, K.; Rendell, A. P.; Burant, J. C.; Iyengar, S. S.; Tomasi, J.; Cossi, M.; Millam, J. M.; Klene, M.; Adamo, C.; Cammi, R.; Ochterski, J. W.; Martin, R. L.; Morokuma, K.; Farkas, O.; Foresman, J. B.; Fox, D. J. *Gaussian 16, Revision C.01*; Gaussian, Inc.: Wallingford, CT, 2019.
(42) (a) Clark, T.; Chandrasekhar, J.; Spitznagel, G. W.; Schleyer, R. v. P. Efficient Diffuse Function-augmented Basis Sets for Anion Calculations. III. The 3-21+G Basis Set for First-Row Elements, Li-F. *J. Comput. Chem.* **1983**, *4*, 294−301. (b) Ditchfield, R.; Hehre, W. J.; Pople, J. A. Self-Consistent Molecular-Orbital Methods. IX. An Extended Gaussian-Type Basis for Molecular-Orbital Studies of Organic Molecules. *J. Chem. Phys.* **1971**, *54*, 724−728. (c) Hariharan, P. C.; Pople, J. A. The Influence of Polarization Functions on Molecular Orbital Hydrogenation Energies. *Theor. Chim. Acta* **1973**, *28*, 213−222. (d) Hehre, W. J.; Ditchfield, R.; Pople, J. A. Self—Consistent Molecular Orbital Methods. XII. Further Extensions of Gaussian—Type Basis Sets for Use in Molecular Orbital Studies of Organic Molecules. *J. Chem. Phys.* **1972**, *56*, 2257−2261.
(43) Dunning, T. H., Jr. Gaussian Basis Sets for use in Correlated Molecular Calculations. I. The Atoms Boron through Neon and Hydrogen. *J. Chem. Phys.* **1989**, *90*, 1007−1023.
(44) Chen, Z.; Wannere, C. S.; Corminboeuf, C.; Puchta, R.; Schleyer, P. v. R. Nucleus-Independent Chemical Shifts (NICS) as an Aromaticity Criterion. *Chem. Rev.* **2005**, *105*, 3842−3888.
(45) Herges, R.; Geuenich, D. Delocalization of Electrons in Molecules. *J. Phys. Chem. A* **2001**, *105*, 3214−3220.


https://doi.org/10.1021/acs.joc.2c01859
*J. Org. Chem.* 2022, 87, 16276−16296